

# Implementation and Learning of Quantum Hidden Markov Models

Vanio Markov,<sup>1</sup> Vladimir Rastunkov,<sup>2</sup> Amol Deshmukh,<sup>2</sup> Daniel Fry,<sup>2</sup> and Charlee Stefanski<sup>1</sup>

<sup>1</sup>*Wells Fargo*

<sup>2</sup>*IBM Quantum, IBM Research*

(Dated: October 7, 2024)

In this article, we apply the theory of quantum channels and open-system state evolution to propose a unitary parameterization and an efficient learning algorithm for Quantum Hidden Markov Models (QHMMs). We consider any quantum channel with a non-trivial operator-sum representation as a stochastic system with hidden dynamics and measurable emissions. By leveraging the richer dynamics of quantum channels, particularly through mixed states, we demonstrate the greater efficiency of quantum stochastic generators compared to classical ones. Specifically, we prove that a stochastic process can be simulated within a quantum Hilbert space using quadratically fewer dimensions than in a classical stochastic vector space.

To provide an implementation of QHMMs within the circuit computing model on quantum hardware, we employ Stinespring’s dilation construction. We show that any QHMM can be efficiently implemented and simulated using a quantum circuit with mid-circuit measurements. A key advantage for feasible QHMM learning in the hypothesis space of unitary circuits lies in the continuity of Stinespring’s dilation. Specifically, if the unitary parameterizations of channels are close in the operator norm, the corresponding channels will be close in both diamond norm and Bures distance. This property forms the foundation for defining of efficient learning algorithms with continuous fitness landscapes.

By employing the unitary parameterization of QHMMs, we establish a formal generative learning model. This model formalizes the empirical distributions of target stochastic process languages, defines the hypothesis space of quantum circuits, and introduces an empirical stochastic divergence measure—hypothesis fitness—as a criterion for learning success. We demonstrate that the learning model features a smooth search landscape, attributable to the continuity of Stinespring’s dilation. The smooth mapping between the hypothesis and fitness spaces facilitates the development of efficient heuristic and gradient descent algorithms.

We consider four examples of stochastic process languages and train QHMMs with hyperparameter-adaptive evolutionary search and multi-parameter nonlinear optimization technique applied to parameterized quantum ansatz circuits. We confirm our results by running optimal circuits on quantum hardware.

## CONTENTS

I. Introduction	2	A. Empirical Specification of Stochastic Languages	16
II. Preliminaries	3	B. QHMM Hypotheses Space	18
A. Stochastic Languages and Hidden Markov Models	3	C. Quality of a Hypothesis	19
B. Quantum States, Measurements, and Quantum Operations	5	1. Precision of a Hypothesis	19
1. Quantum States	5	2. Complexity of a Hypothesis	20
2. Quantum Measurements	6	D. Formalization of the QHMM Learning Problem	20
3. Quantum Evolution	7	E. QHMM Learning Algorithm	23
4. Composite Systems	8	F. Learning QHMM with Ansatz Circuits	27
III. Quantum Hidden Markov Models	9	G. Ansatz Circuit Template	28
A. Unitary Definition of QHMM	11	V. Examples of QHMMs	28
B. Primary and Measurement System Design. Test Case for the Circuit Ansatz Design	14	A. Simple Four Symbol Stochastic Process	28
IV. Learning Quantum Hidden Markov Models	16	B. Classic Market Model with Four Hidden States	31
		VI. Conclusions and Outlook	32
		VII. Acknowledgements	32
		References	33

## I. INTRODUCTION

In this article, we study quantum models of discrete stochastic processes. We assume these processes are generated by finitary mechanisms with limited memory and time. Additionally, only a subset of the process variables is observable, while the distributions of these observations depend on an underlying unobservable process. A common approach to modeling such systems involves two joint stochastic processes: a latent state process and a dependent output emission process. The state process is treated as a finite-state Markovian process [1], where the states are ‘hidden’. The observable process is defined as a probabilistic mapping from the hidden states to the symbols of a finite alphabet. This modeling framework is commonly known as a *Hidden Markov Model* (HMM) [2].

Hidden Markov Models have broad applications in various real-world domains. The concept of latent variables enables the estimation of unobservable circumstances and relationships, while the assumption of underlying Markovian dynamics allows for the development of efficient learning and inference procedures. Originally introduced by Baum and Petri in 1966 [3] HMMs have since been successfully applied in fields such as linguistics [4–7], DNA analysis [8–10], engineering [11, 12], and finance [2, 13].

The *learning problem* for HMMs involves estimating the transition and emission operators of an unknown HMM from a finite sample of its emission distributions. The conventional approach to solving this problem is through maximizing the likelihood of the observations [3, 14–17]. Although the expectation-maximization (EM) algorithm used for this task cannot be performed in polynomial time [18], it has been widely successful in practice [19]. Another class of learning algorithms, known as *spectral algorithms* [20–22] has polynomial time complexity. These algorithms represent the joint frequencies of observed sequences as a Hankel matrix [20], whose rank provides an estimate of the model’s order. The model parameters are then derived from the factors of the matrix’s singular value decomposition. These spectral learning algorithms are part of a specialized field known as the *realization problem* for HMMs [20, 21].

The objective of this research is to propose a methodology for the physical implementation of Quantum HMMs and to develop practical learning algorithms. Our approach involves *quantizing* a classical HMM by replacing its stochastic vector space with the space of quantum density operators. The classical transition and emission operators are mapped to *observable operators* [23], which are then replaced by *quantum operations*. A quantum

operation, also known as a *quantum channel*, is a linear, completely positive trace-preserving (CPTP) map defined on the space of density operators [24]. When used to quantize a classical HMM, a quantum operation serves two roles. First, it defines the stochastic evolution of the model’s state, representing the underlying Markovian process. Second, when interpreted as a *positive operator-valued measure* (POVM), the quantum operation describes the observable process.

The definition of a Quantum Hidden Markov Model (QHMM) as a quantum operation was initially introduced by Monras et al. [25]. Since then, various aspects of QHMMs have been explored by Srinivasan et al. [26–32], O’Neill [33], and Clark [34]. Javidian [35] discussed a different type of model called the circular QHMM. Cholewa et al. [36] studied HMMs based on quantum walks and transition operation matrices. Elliot [37] demonstrated that QHMMs offer a distinct advantage over their classical counterparts through the use of memory compression. This compression relates to the reduced size of the model’s state space and the amount of information it stores. Additionally, other quantum approaches to modeling discrete stochastic processes have been proposed. For instance, Blank et al. [38] investigated the characteristic function of discrete stochastic processes and introduced a quantum algorithm for learning it, utilizing techniques such as quantum amplitude estimation and quantum Monte Carlo methods.

Assuming a QHMM is defined as a quantum channel, we explore its implementation as a quantum circuit with mid-circuit measurements using Stinespring’s dilation theorem [39]. Additionally, we leverage the continuity of Stinespring’s construction [40] to define a hypothesis space and a corresponding learning objective, enabling efficient learning of QHMMs.

The main contributions of our research are:

- We demonstrate that QHMMs provide a more efficient description of discrete stochastic processes in terms of state-space complexity compared to classical HMMs. Specifically, we show that for every classical HMM of order  $n$ , there exists a QHMM of order  $N = \sqrt{n}$  which generates the same stochastic process language.
- For every QHMM defined as a quantum operation we provide an equivalent QHMM implementation as a unitary circuit with mid-circuit measurement.
- We provide a formal QHMM learning model formalizing the training data sample, hypothesis space of unitary quantum circuits, and

hypothesis quality criteria as stochastic divergence between two distributions.

- We propose a tractable empirical distance measure between two QHMMs in terms of the divergence of their observable distributions. We prove that the empirical distance is dominated by the distance measure induced on the space of QHMMs by the diamond norm.
- We prove that the landscape of the proposed QHMM learning model is smooth resulting from the continuity and convergence properties of Stinespring’s dilation theorem [40]. The smooth landscape implies efficient heuristic and gradient-based learning algorithms.
- We specify a QHMM learning algorithm as adaptive evolutionary search in the space of quantum circuits with mid-circuit measurement.
- We specify a QHMM learning algorithm as multi-parameter nonlinear optimization in the space of pre-defined quantum ansatz.

This article is organized as follows:

- Section II presents some preliminary information regarding stochastic process languages, classic hidden Markov models and observable operators models. It introduces critical concepts including quantum states, quantum operations, general measurement and quantum mid-circuit computation.
- Section III presents the basic definition of a QHMM as quantum operation and provides unitary definition of QHMMs and their implementation as quantum circuits with mid-circuit measurement.
- Section IV discusses a formal QHMM learning model defining data samples, hypothesis space and learning criterion. It specifies adaptive evolutionary and ansatz-based QHMM learning algorithms.
- Section V presents two examples: a market model and a stochastic volatility model.
- Section VI discusses our conclusion and outlook.

## II. PRELIMINARIES

### II.A. Stochastic Languages and Hidden Markov Models

We study a class of discrete time stationary stochastic processes,

$$\{Y_t : t \in \mathbb{N}, Y_t \in \Sigma\}, \quad (1)$$

where  $\Sigma = \{a_1, \dots, a_m\}$  is a finite set of observable symbols, called an *alphabet*. The set of all finite sequences over the alphabet  $\Sigma$ , including the empty sequence  $\epsilon$ , is denoted by  $\Sigma^*$ . Finite sequences of symbols are denoted by the bold lowercase letters  $\mathbf{a}$ ,  $\mathbf{p}$ ,  $\mathbf{s}$ . The set of all sequences with length exactly  $t$  is denoted by  $\Sigma^t$ . For any  $\mathbf{a} \in \Sigma^*$  let  $|\mathbf{a}|$  be the number of symbols in the sequence. If  $\mathbf{p}$  and  $\mathbf{s}$  are sequences, then  $\mathbf{ps}$  denotes their *concatenation*. The sequence  $\mathbf{p}$  is called the *prefix* and  $\mathbf{s}$  is called the *suffix* of  $\mathbf{ps}$ . Any subset of  $\Sigma^*$  is a *language*  $L$  over the alphabet. The sequences belonging to a language are referred to as *words*. The set of sequences originated by observations or measurement of the evolution of a discrete-time process is called the *process language*. It is easy to verify that if a word results from the observation of a process, then every one of its subwords has also been observed. Therefore, the process languages are *subword-closed*.

A *stochastic process language*  $L$  is a process language together with a set

$$D^L = \{D_t^L : t \geq 0\} \quad (2)$$

of finite dimensional probability distributions  $D_t^L$ , each of which is defined on the sequences with length exactly  $t$ :

$$D_t^L = \left\{ P[\mathbf{a}] : \mathbf{a} \in \Sigma^t, \sum_{\mathbf{a} \in \Sigma^t} P[\mathbf{a}] = 1 \right\} \quad (3)$$

It is easy to verify that the set of subwords of every realization of a stationary stochastic process (1) is a stochastic process language.

We will assume that each observation  $Y_t$  in the process (1) depends on the state of a non-observable or *hidden* finite-state process  $\{X_t : X_t \in S\}$ , where  $S = \{s_1 \dots s_n\}$ . The processes  $\{Y_t\}$  and  $\{X_t\}$  are called *emission process* and *state process* respectively. If the joint process  $\{Y_t, X_t : t \in \mathbb{N}, Y_t \in \Sigma, X_t \in S\}$  is stationary, then we can describe it by a linear model known as (classical) Hidden Markov Model (HMM). The model defines *Markovian* evolution of the hidden state process  $\{X_t\}$ . The observed process  $\{Y_t\}$  is emitted by a linear stochastic operator mapping the current hidden state to an observable symbol.

**Definition 1** (Classical Hidden Markov Model). A classical hidden Markov model is defined as a 5-tuple:

$$\mathbf{M} = \{\Sigma, S, A, B, \mathbf{x}_0\}$$

where  $\Sigma = \{a_1 \dots a_m\}$  is a finite set of observable symbols,  $S = \{s_1 \dots s_n\}$  is a finite set of unobservable or hidden states and the number of states  $n$  is called the order of the model,  $A$  is a column-stochastic state transition matrix,  $B$  is a row-stochastic observations emission matrix, and  $\mathbf{x}_0$  is a stochastic vector defining the initial superposition of process' states.

At any moment in time  $t$ , the model is in a superposition (stochastic mixture) of its hidden states, described by a stochastic vector  $x_t \in \mathbb{R}^n$ . The component  $x_t^i$  represents the probability of being in state  $s_i$ . The evolution of the hidden states follows a Markovian process defined by the transition matrix:

$$x_{t+1} = Ax_t.$$

At any moment in time  $t$ , the model defines symbol emission probabilities using a stochastic vector  $y_t \in \mathbb{R}^m$ , which depends on the current state  $x_t$  through the emission matrix  $B$ :

$$y_t = Bx_t.$$

The component  $y_t^i$  represents the probability of emitting symbol  $a_i$  at moment  $t$ . It's important to note that the evolution of the observation process, in general, is not a Markovian process.

The *steady state* of a stationary HMM is a stochastic vector  $\mathbf{x}^*$  defined as

$$\mathbf{x}^* = A\mathbf{x}^*.$$

The steady state  $\mathbf{x}^*$  is the eigenvector of the state transition operator  $A$  with eigenvalue 1, normalized to represent a probability distribution.

For every HMM  $\mathbf{M}$  we can define a set of *observable operators*  $\mathbf{T}$  as

$$\mathbf{T} = \{T_a : T_a = AB_a, a \in \Sigma\} \quad (4)$$

where  $B_a = \text{diag}(B[a, i]), i \in 1..n$  are diagonal matrices defining symbol observation probabilities for each state  $s_i$  [41, 42].

Each element of the observable operator  $T_a$  defines the conditional probability that the model is in state  $s_i$  and emits symbol  $a$ , given that it was in state  $s_j$  at the previous time step.

$$T_a^{i,j} = P[s_j | s_i, a].$$

Let  $\mathbf{a} = a_1 \dots a_t$  be any sequence. We define the observable operator corresponding to  $\mathbf{a}$  as follows:

$$T_{\mathbf{a}} = T_{a_1} \dots T_{a_t}.$$

For any sequences  $\mathbf{a}, \mathbf{b} \in \Sigma^*$  the following composition of the observable operators is easy to verify:

$$T_{\mathbf{ab}} = T_{\mathbf{a}}T_{\mathbf{b}}.$$

The state transition operator  $A$  is related to the observable operators  $\{T_a\}$  as follows:

$$A = \sum_{a \in \Sigma} T_a.$$

A Hidden Markov Model (HMM)  $\mathbf{M}$  defines the probability of every finite observable sequence  $\mathbf{a} = a_1 \dots a_t$  as:

$$P[\mathbf{a}|\mathbf{M}] = \mathbf{1}T_{a_t} \dots T_{a_1}\mathbf{x}_0 = \mathbf{1}T_{\mathbf{a}}\mathbf{x}_0, \quad (5)$$

where  $\mathbf{1}$  is the unit row vector with dimension  $n$ . With every model  $\mathbf{M}$  we associate a *sequence function*  $f^{\mathbf{M}} : \Sigma^* \rightarrow [0, 1]$  defined as:

$$f^{\mathbf{M}}(\mathbf{a}) = P(\mathbf{a}|\mathbf{M}), \forall \mathbf{a} \in \Sigma^*. \quad (6)$$

Through its sequence function, every HMM  $\mathbf{M}$  defines a stochastic process language  $L^{\mathbf{M}}$  consisting of a set of distributions for each  $t \in \mathbb{N}$ :

$$D_t^{\mathbf{M}} = \{f^{\mathbf{M}}(\mathbf{a}) : \mathbf{a} \in \Sigma^t\} \quad (7)$$

We compare HMMs based on the languages they define or generate. Two HMMs are considered *equivalent* if they define the same stochastic process language.

Let us assume that we have observed a process up to a certain moment in time  $t$ :

$$\mathbf{a} = a_1 \dots a_t.$$

The probability of the next symbol being  $a$  is given by:

$$\begin{aligned} P[a|\mathbf{a}] &= \frac{P[\mathbf{a}a]}{P[\mathbf{a}]} \\ &= \mathbf{1}T_a \frac{T_{\mathbf{a}}\mathbf{x}_0}{\mathbf{1}T_{\mathbf{a}}\mathbf{x}_0} \\ &= \mathbf{1}T_{\mathbf{a}}\mathbf{x}_t, \end{aligned}$$

where

$$\mathbf{x}_t = \frac{T_{\mathbf{a}}\mathbf{x}_0}{\mathbf{1}T_{\mathbf{a}}\mathbf{x}_0}$$

is the stochastic mixture of states after the emission of the sequence  $\mathbf{a} = a_1 \dots a_t$ .

For every HMM  $\mathbf{M}$ , let's consider a *bi-infinite* matrix, commonly referred to as a generalized *Hankel matrix*, defined by the sequence function (6) of the model [43]:

$$H^{\mathbf{M}} \in R^{\Sigma^* \times \Sigma^*}, H^{\mathbf{M}}[\mathbf{p}, \mathbf{s}] = f^{\mathbf{M}}(\mathbf{ps}), \forall \mathbf{p}, \mathbf{s} \in \Sigma^*, \quad (8)$$

where  $\mathbf{ps}$  denotes a concatenation of sequences  $\mathbf{p}$  and  $\mathbf{s}$ . We can say that  $H^{\mathbf{M}}$  is indexed by the prefix  $\mathbf{p}$  and suffix  $\mathbf{s}$  of the sequence  $\mathbf{ps}$ . The rows of  $H^{\mathbf{M}}$  are indexed by the prefixes  $\mathbf{p}$  in the *first lexicographical order*, and the columns are indexed by suffixes  $\mathbf{s}$  in the *last lexicographical order* of the sequences [43]. A sequence function  $f^L$  and the corresponding generalized Hankel matrix  $H^L$  are defined for every stationary stochastic language  $L$  by the distributions  $D_t^L$  (3):

$$f^L(\mathbf{a}) = P[\mathbf{a}|D_t^L], \forall \mathbf{a} \in \Sigma^t, \forall t \in \mathbb{N}. \quad (9)$$

The *rank* of a stochastic language is the rank of its Hankel matrix. This matrix is important, because its finite-rank property is a necessary condition for the stochastic language to have a HMM realization.

**Theorem 1** (Anderson [43]). *If  $H^{\mathbf{M}}$  is the infinite generalized Hankel matrix associated with a HMM  $\mathbf{M}$  of order  $n$ , then  $\text{rank}(H^{\mathbf{M}}) \leq n$ .*

It has been proven [44], that the equality in **Theorem 1** can be reached, i.e. there are minimal order HMMs with  $\text{rank}(H^{\mathbf{M}}) = n$ . If a HMM  $\mathbf{M}$  has order  $n$  its finite dimensional distributions  $D_t^{\mathbf{M}}$  are completely defined by the values of the sequence function  $f^{\mathbf{M}}(\mathbf{a})$  for all sequences  $\mathbf{a}$  of length at most  $2n - 1$  [41, 42].

In general, not every finite-rank stochastic language has a HMM [45]. Furthermore, determining whether a stochastic language  $L$  has finite rank is an undecidable problem [46].

**Example 1.** The evolution of asset prices on today's exchanges is driven by the interaction of ask and bid orders placed on an electronic two-sided queue known as a *Limit Order Book* (LOB) [47]. One important statistic associated with the LOB is the *mid-price*. The mid-price is the mean of lowest ask order price and highest bid order price at any given moment. In this example we present very simple HMM of the discrete-time mid-price direction of change.

At any given moment, the symbol  $\mathbf{1}$  is observed if the price has increased, while the symbol  $\mathbf{0}$  is observed if the price has decreased or remained unchanged. It is assumed that the distribution of observed directions of change depends on the underlying state of the market, which is not directly observable. Let's consider a very simple situation, where the market can be in one of four states: bear, bull, transition to bear, or transition to bull, as listed in Table I. The distribution of observation sequences is depicted in FIG 1. The generalized Hankel matrix associated with the model has a rank of 4 for sequences containing up to 20 symbols. Therefore, we conclude that the order of this model is 4.

## II.B. Quantum States, Measurements, and Quantum Operations

We study quantum models of discrete-time joint stochastic processes. These models assume two processes: an underlying, hidden Markov process that evolves in discrete time according to linear stochastic dynamics, and a second, observable process that produces an observation at each time step by applying a stochastic map to the hidden state. To quantize this model, it is necessary to define quantum concepts that correspond to its states, observables, and state evolution.

### II.B.1. Quantum States

The states of the process will be represented by the states of an  $n$ -qubit quantum system, where the associated complex Hilbert space  $\mathcal{H}$  [24] is a linear vector space with an inner product and dimension  $N = 2^n$ . The vectors of  $\mathcal{H}$  are denoted by  $|v\rangle$ . A complete description of the quantum system at any given moment in time is called a *quantum state*. When a quantum state is precisely determined, it is a *pure state*. A pure state is defined by a vector  $|v\rangle$  with unit norm  $\langle v|v\rangle = 1$ . To give a probabilistic interpretation of the pure states let's assume that  $\{|x\rangle\}$  is an orthonormal basis in  $\mathcal{H}$  and any pure state  $|v\rangle$  can be represented as

$$|v\rangle = \sum_x a_x |x\rangle. \quad (10)$$

The coefficients  $a_x$  are called amplitudes and the sum of the squares of their modules is normalized:

$$\langle v|v\rangle = \sum_x |a_x|^2 = 1$$

The square of the magnitude of the amplitude  $a_x$  corresponds to the probability of observing the system in the classical state  $|x\rangle$ :

$$P[|x\rangle | |v\rangle] = \langle x|v\rangle = \langle v|P_x|v\rangle, \quad (11)$$

where  $P_x$  is the projector onto the subspace  $|x\rangle$ .

When we consider open quantum systems exchanging information or focus on subsystems of a composite quantum system the quantum state becomes statistically uncertain. The uncertainty in the quantum states is described by statistical mixtures of pure states, each occurring with specified probability. This ensemble is known as a *mixed state*. To describe pure and mixed states in one mathematical framework we use *density operators* which are

$s$	Description
0	Bear - Tendency down
1	Bull - Tendency up
2	Transition to Bear
3	Transition to Bull

$s$	0	1	2	3
0	0.5	0.1	0.15	0.25
1	0.1	0.5	0.25	0.15
2	0.25	0.15	0.5	0.1
3	0.15	0.25	0.1	0.5

$s$	Symbol 0	Symbol 1
0	0.8	0.2
1	0.2	0.8
2	0.4	0.6
3	0.6	0.4

TABLE I. Left: Market hidden states descriptions. Center: State transition probabilities. Right: Observed symbol probabilities.

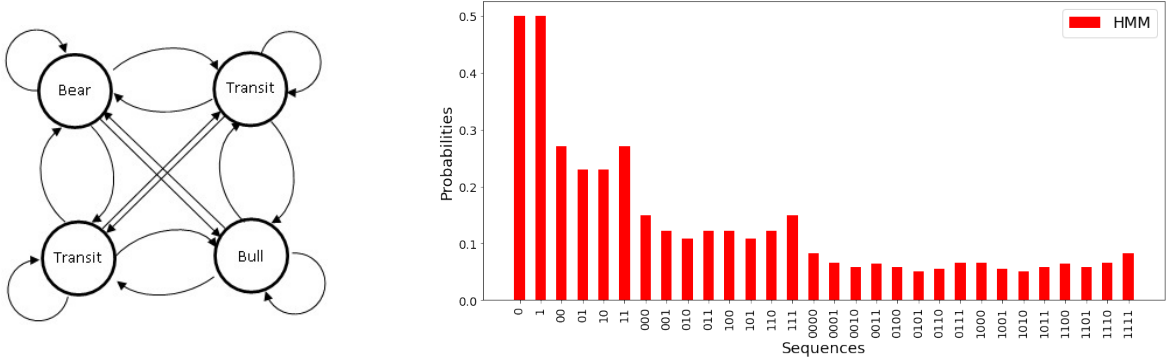


FIG. 1. Left: State transition graph. Right: Distribution of observed symbol sequences.

weighted sums of the pure states (10) projectors:

$$\rho = \sum_v p_v \rho_v, \quad \sum_v p_v = 1. \quad (12)$$

Here,  $p_v$  represents the probability of the system to be in the pure state  $|v\rangle$ , and the sum of all these probabilities is equal to 1. The projector

$$\rho_v = |v\rangle \langle v|$$

is the density operator of the pure state  $|v\rangle$ . The density operators of pure states satisfy the equation  $\rho_v = \rho_v^2$  and they form a complex projective space. In other words, they are projectors onto the one-dimensional subspaces of  $\mathcal{H}$ .

The density operator provides a complete and compact description of the mixed state, encoding all the essential statistics (probabilities and coherences) even when the ensemble contains more pure states than the dimension of the Hilbert space. Formally, a density operator  $\rho$  is a *bounded linear operator* with the following properties:

1.  $\rho$  is *Hermitian*, i.e.  $\rho = \rho^\dagger$ .
2.  $\rho$  is a non-negative definite:  $\langle v|\rho|v\rangle \geq 0$ ,  $\forall |v\rangle \in \mathcal{H}$ .
3.  $\rho$  has unit trace:  $\text{tr}(\rho) = 1$ .
4. The eigenvalues  $\lambda_1, \dots, \lambda_N$  of  $\rho$  form a probability distribution.

The space of pure and mixed states forms a *convex* subspace within the Hilbert space  $\mathcal{H}$ . The extreme points of this subspace are the pure states, while the mixed states are considered as points within this convex subspace.

We will denote the space of bounded linear operators on the Hilbert space  $\mathcal{H}$  by  $B(\mathcal{H})$ , the space of Hermitian operators by  $H(\mathcal{H})$  and the space of corresponding density operators by  $D(\mathcal{H})$ . The space  $H(\mathcal{H})$  is a linear vector space, but  $D(\mathcal{H})$  is not. A general linear combination of density operators is Hermitian, but its trace is not necessarily equal to one. The space of density operators  $D(\mathcal{H})$  forms an  $N^2 - 1$  - dimensional convex space which embeds in  $H(\mathcal{H})$  [48].

### II.B.2. Quantum Measurements

We extract classical information about a quantum state through observation or measurement. The measurement of an observable is modeled by a Hermitian (self-adjoint) operator acting on the quantum state. In the most general case, if an observable has  $k$  classical measurement outcomes  $\{m_1, \dots, m_k\}$ , the corresponding measurement operator  $M$  is a set of  $k$  positive semidefinite operators  $M_i$  which is a complete set:



$$M = \{M_i\}_{i=1}^k, \quad (13)$$

$$\sum_{i=1}^k M_i = I.$$

The probability of outcome  $m_i$  in state  $\rho$  is

$$P[m_i|\rho] = \text{tr}(M_i\rho), \quad (14)$$

and the normalized state after observing outcome  $m_i$  is defined by

$$\rho_i = \frac{M_i\rho}{P[m_i|\rho]}. \quad (15)$$

### II.B.3. Quantum Evolution

Classical Hidden Markov Models use linear operators to describe the stochastic evolution of states. Similarly, in discrete-time quantum systems, state transformations are defined by linear operators known as quantum operations. A quantum operation, denoted by  $\mathcal{O}$ , is a linear map:

$$\mathcal{O} : B(\mathcal{H}) \rightarrow B(\mathcal{H})$$

with the following properties:

1.  $\mathcal{O}$  preserves convex structure of density operators. If the map is applied to a stochastic ensemble of density operators, then the outcome is the same ensemble of the resulting densities.
2.  $\mathcal{O}$  is trace preserving:

$$\text{tr}(\mathcal{O}\rho) = \text{tr}(\rho), \forall \rho \in B(\mathcal{H})$$

This property ensures the conservation of probability in physical processes.

3.  $\mathcal{O}$  is a *completely positive* map. Furthermore, it remains positive under any tensor product extension, meaning that  $(\mathcal{O} \otimes I_k)$  is positive for all  $k > 0$ .

These properties ensure that a quantum operation is a valid and consistent evolution of quantum states, preserving the probabilistic nature and positivity of density operators.

According to these properties a quantum operation is a Completely Positive Trace-Preserving (CPTP) linear map, which defines the evolution of a discrete-time quantum system. In this context, a quantum operation is often called a *quantum channel*.

An simple example of quantum operation is the evolution of the density operator under a unitary transformation  $U$ :

$$\mathcal{O}_U\rho = U\rho U^\dagger. \quad (16)$$

Another example is the general measurement discussed in the previous section. We can decompose every positive semidefinite operator  $M_i$  as  $M_i = E_i^\dagger E_i$ , and represent the observable as follows:

$$M\rho = \sum_{i=1}^k E_i\rho E_i^\dagger. \quad (17)$$

Any quantum operation  $\mathcal{O}$  can be expressed as an operator-sum representation as follows:

$$\mathcal{O}\rho = \sum_e K_i\rho K_i^\dagger, \quad (18)$$

where the operators  $\{K_i\}$ , known as *Kraus operators* satisfy requirements related to the properties of a CPTP map:

1. Kraus operators are linear operators
  2. To ensure that  $\mathcal{O}$  is trace-preserving the completeness constraint should be satisfied:
- $$\sum_i K_i = I. \quad (19)$$
3. To ensure that  $\mathcal{O}$  is complete positive the Kraus operators should map positive semi-definite matrices to positive semi-definite matrices.

A quantum operation can be represented by different number of Kraus operators but there is a minimum. The minimal integer  $k$  for which the operation  $\mathcal{O}$  has decomposition with  $k$  operators is called *Kraus rank* of the operation  $\mathcal{O}$  denoted by  $\text{rank}(\mathcal{O})$ . The Kraus rank is equal to the rank of a positive linear operator known as *Choi matrix* [49] of the operation. The Kraus rank of an operation varies from 1 for unitary transformations to  $N^2$  for completely depolarizing operations. The set of quantum operations is a convex set with dimension  $N^4 - N^2$ . The extreme points of the set are operations defined by linearly independent Kraus operators  $\{K_i\}$  with maximal rank  $N$  [49]. Every quantum operation can be represented as convex combination of  $N^2$  extreme operations. The specific Kraus operators in the operator-sum decomposition are not unique, but different sets of Kraus operators for the same quantum operation are related by a unitary transformation.

The operator-sum representation provides a dual interpretation of quantum operations. First, it describes the classical-quantum dynamics of state evolution, as expressed by equation (18). The application of each Kraus operator  $K_i$  results in a new quantum state:

$$\rho_i = \frac{K_i \rho K_i^\dagger}{P[\rho_i|\rho]}, \quad (20)$$

where the probability for transition to state  $\rho_i$  is

$$P[\rho_i|\rho] = \text{tr}(K_i \rho K_i^\dagger). \quad (21)$$

Second, it defines a Positive Operator-Valued Measure (POVM) observable. The complete set of Kraus operators (19) can be interpreted as outcomes of a general measurement observable (13). For every Kraus operator  $K_i$  we define a quantum operation  $V_i$  acting on the state  $\rho$  as follows:

$$V_i \rho = K_i \rho K_i^\dagger. \quad (22)$$

The operations  $V_i = K_i^\dagger K_i$  are Hermitian and positive. They satisfy the completeness property  $\sum_i V_i = I^N$ , since the quantum operation  $\mathcal{O}$  defined in (18) is trace-preserving:

$$\text{tr}(\mathcal{O}\rho) = \text{tr}\left(\sum_i V_i \rho\right) = 1. \quad (23)$$

The operators  $\{V_i\}$  define a generalized measurement observable  $V$  as specified in (13). The probability of outcome  $i$  in state  $\rho$  is

$$P[i|\rho] = \text{tr}(V_i \rho), \quad (24)$$

and the normalized state after observing outcome  $i$  is defined by

$$\rho_i = \frac{V_i \rho}{P[i|\rho]}. \quad (25)$$

#### II.B.4. Composite Systems

Our goal is to model the joint processes of hidden state evolution and observations. To achieve this, we will consider *bipartite* quantum systems. The evolution of the hidden state is modeled by the dynamics of a quantum system with Hilbert space  $\mathcal{H}_S$ , dimension  $N$ , and an orthonormal basis  $\{|s\rangle\}$ . This quantum system, referred to as the “state” or  $S$ -system, represents the underlying dynamics of the stochastic process.

The process of observable symbol emission, which depends on the hidden state, is modeled by a second quantum system, the *emission* or  $E$ -system. This system has Hilbert space  $\mathcal{H}_E$ , dimension  $M$ , and an orthonormal basis  $\{|e\rangle\}$ . The dimension  $M$  of the emission system is equal to or greater than the number of observable symbols in the stochastic process.

To represent the quantum system composed of these two subsystems, we employ a quantum operation that combines the components through a tensor product, forming a bipartite quantum system.

$$\rho_S \mapsto \rho_S \otimes \rho_E = \rho_{SE}, \quad (26)$$

where the composed Hilbert space is

$$\mathcal{H}_{SE} = \mathcal{H}_S \otimes \mathcal{H}_E. \quad (27)$$

Here the state  $\rho_{SE}$  is a *tensor product state*, i.e. initially the subsystems are not entangled. A further assumption is that the initial state of the emission component is a fixed pure state  $\rho_E = |e_0\rangle\langle e_0|$ , where  $|e_0\rangle \in \{|e\rangle\}$ .

In order to describe one of the components of a bipartite system while disregarding the other we use a quantum operation known as *partial trace* [24]. The partial trace operation is a linear transformation that maps the density operator of the bipartite system to the *reduced density* operator of one of the components:

$$\begin{aligned} \mathcal{O}\rho_{SE} &= \text{tr}_E(\rho_S \otimes \rho_E) \\ &= \sum_e (I_N \otimes \langle e|) (\rho_S \otimes \rho_E) (I_N \otimes |e\rangle) \\ &= \rho_S \end{aligned} \quad (28)$$

The partial trace operation in (28) is applied to a non-entangled bipartite system and therefore the partial density of the state system is independent from the emission system. To model joint stochastic processes a unitary operation (16) is applied to entangle the subsystems and transfer information from the hidden state to the observable:

$$\mathcal{O}_U \rho_{SE} = U \rho_{SE} U^\dagger. \quad (29)$$

The evolution of the hidden state is described by tracing out the emission component (28):

$$\begin{aligned} \text{tr}_E(\mathcal{O}_U \rho_{SE}) &= \text{tr}_E(U \rho_{SE} U^\dagger) \\ &= \text{tr}_E(U (\rho_S \otimes |e_0\rangle\langle e_0|) U^\dagger) \\ &= \sum_e K_e \rho_S K_e^\dagger. \end{aligned} \quad (30)$$

where

$$K_e = (I^N \otimes \langle e|) U (I^N \otimes |e_0\rangle). \quad (31)$$



The equation (30) defines operator-sum representation of the quantum operation  $\mathcal{O}_U$ . The Kraus operators depend on the unitary  $U$ , and the arbitrary selected orthonormal basis  $\{|e\rangle\}$  of the emission system. Since any unitary transformation of a basis is also an orthonormal basis, the operator-sum representation is defined up to a unitary transformation.

We have demonstrated that, although an entangled bipartite system is in a pure state, the individual states of its “state” and “emission” components exhibit characteristics similar to mixed states when observed independently or described using the partial trace operation. This property of the bipartite system is significant, as it enables the use of density operators to model classical stochastic states, despite the underlying pure quantum nature of the system.

A mixed state of one component in an entangled bipartite pure state can also be defined by performing a projective measurement on the other component. The measurement outcome on the “emission” component provides information about the state of the “state” component, due to the entanglement between the two components. Let  $\{|e\rangle\}$  be an orthonormal basis of the emission component. The corresponding set of orthogonal projectors is:

$$\{M_e = |e\rangle\langle e|, e = 0, \dots, M-1\}.$$

We can extend this set to operators  $\{P_e\}$  acting on the bipartite system:

$$P_e = I_N \otimes M_e.$$

The measurement operation on the full system is defined as (17):

$$M\rho_{SE} = \sum_e P_e \rho_{SE} P_e^\dagger.$$

When we first apply the unitary  $U$  to the bipartite system and then measure the emission component the resulting state is

$$\rho' = P_e U(\rho_S \otimes \rho_E) U^\dagger P_e^\dagger$$

Using the definition of Kraus operators (31) and the measurement outcomes  $V_e$  defined as Kraus operators (22) we have :

$$\rho' = K_e \rho_S K_e^\dagger = V_e \rho_S$$

The measurement outcomes after the unitary operation have probabilities defined in (14):

$$P[e | U\rho_{SE}U^\dagger] = \text{tr}(V_e \rho_S) \quad (32)$$

We can summarize that in a bipartite system  $\rho_{SE} = \rho_S \otimes \rho_E$  the operation of entanglement of

the components, followed by tracing out of one component, e.g.  $\rho_E$ , has the same operator-sum representation and outcomes probability distribution as a unitary entanglement of the bipartite system followed by projective measurement of the emission component and “discarding” the outcome. Both cases are equivalent to a POVM operation on  $\rho_S$  as defined in (22):

$$\begin{aligned} \text{tr}_E(\mathcal{O}_U \rho_{SE}) &= \sum_e (P_e U(\rho_S \otimes \rho_E) U^\dagger P_e^\dagger) \\ &= \sum_e K_e \rho_S K_e^\dagger = \sum_e V_e \rho_S \quad (33) \\ &= M(\mathcal{O}_U \rho_{SE}). \end{aligned}$$

The equality in (33) provides two equivalent approaches for modeling the joint process of a state evolution and dependent symbol emission. It can be represented either as a POVM operation on the state system or as a unitary transformation  $U$  entangling the full system followed by a projective measurement on the emission component. In both cases, the state of the state system  $S$  becomes a mixed state, representing a stochastic ensemble that averages all possible post-measurement states. This behavior reflects the characteristics of classical stochastic generators and allows the quantum model to reflect the probabilistic nature of the joint stochastic process.

### III. QUANTUM HIDDEN MARKOV MODELS

The POVM operations (22) as described in Section II B define a joint stochastic process of quantum state transitions and symbols emission. The quantum operation acting on a quantum state resembles the classical observable operators (4) transforming a classical stochastic state as defined in Section II A. These similarities provide the foundation for the following quantum Hidden Markov Model (QHMM) definition:

**Definition 2** (Quantum Hidden Markov Model [25]). *A Quantum HMM (QHMM)  $\mathbf{Q}$  over an  $N$ -dimensional Hilbert space  $\mathcal{H}$  is a 4-tuple:*

$$\mathbf{Q} = \{\Sigma, \mathcal{H}, \mathcal{T} = \{T_a\}_{a \in \Sigma}, \rho_0\}, \quad (34)$$

where

- $\Sigma$  is a finite alphabet of observable symbols.
- $\mathcal{H}$  is an  $N$ -dimensional Hilbert space with space of density operators  $D(\mathcal{H})$ .
- $\mathcal{T}$  is a CPTP map (quantum channel)  $\mathcal{T} : D(\mathcal{H}) \rightarrow D(\mathcal{H})$ .

- $\{T_a\}_{a \in \Sigma}$  is an operator-sum representation of  $\mathcal{T}$  in terms of a complete set of Kraus operators.
- $\rho_0$  is an initial state,  $\rho_0 \in D(\mathcal{H})$ .

When the operation  $\mathcal{T} = \{T_a\}_{a \in \Sigma}$  is applied to the state  $\rho \in D(\mathcal{H})$ , any symbol  $a \in \Sigma$  will be observed/emitted with probability (24):

$$P[a|\rho] = \text{tr}(T_a \rho)$$

and the system's state will become (25):

$$\rho_a = \frac{T_a \rho}{P[a|\rho]}.$$

If the operation  $\mathcal{T}$  is applied  $t$  times starting at the initial state the model will emit a sequence of symbols  $\mathbf{a} = a_1 \dots a_t$  with probability

$$P[\mathbf{a}|\rho_0] = \text{tr}(T_{\mathbf{a}} \rho_0). \quad (35)$$

where

$$T_{\mathbf{a}} = T_{a_t} \dots T_{a_1}$$

For each QHMM  $Q$  the equation (35) defines a *sequence function*  $f^Q$  and corresponding Hankel matrix (8)  $H^Q$  as follows:

$$f^Q(\mathbf{a}) = P[\mathbf{a}|\rho_0], \forall \mathbf{a} \in \Sigma^*, \quad (36)$$

$$H^Q[\mathbf{p}, \mathbf{s}] = f^Q(\mathbf{ps}), \forall \mathbf{p}, \mathbf{s} \in \Sigma^*. \quad (37)$$

The sequence function (36) defines a distribution  $D_t^Q$  over the sequences of length  $t$  for  $\forall t > 0$ :

$$D_t^Q = \{f^Q(\mathbf{a}) : \mathbf{a} \in \Sigma^t\} \quad (38)$$

Therefore every QHMM  $Q$  defines a *stochastic process language*  $\mathbf{L}^Q$  (2) over the set of finite sequences  $\Sigma^*$ .

The eigenvector  $\rho^*$  of the quantum operation  $\mathcal{T}$  with eigenvalue 1, normalized to represent a distribution, is the *steady state* of the model  $Q$ :

$$\rho^* = \mathcal{T} \rho^*. \quad (39)$$

The dimension of the Hilbert space  $\dim(\mathcal{H}) = N$  is called *order* of the quantum model  $Q$ .

Any iteration of the quantum operation  $\mathcal{T}$ :

$$\rho_t = \mathcal{T}^t \rho_0, t \geq 0, \quad (40)$$

defines a mixed state  $\rho_t$ , which corresponds to all the stochastic paths for generation of a symbol sequence with length  $t$ .

A theorem in [25], demonstrates that QHMMs can generate the class of languages generated by the classic HMMs. The theorem claims that for every classic HMM of order  $N$  there exists a QHMM of the same order which generates the same stochastic process language. It is important to explore whether the quantum framework allows for a more efficient representation of stochastic process languages. Since the states of QHMMs are represented by density operators, it is crucial to estimate the size of a basis of density operators. The space of density operators  $D(\mathcal{H})$  is a closed and bounded convex space with dimension  $N^2 - 1$ . The extreme point of  $D(\mathcal{H})$  are the density operators of the pure states. Extensive study of the geometry of  $D(\mathcal{H})$  is presented for example in [48]. Here we will show that the space of Hermitian matrices  $H(\mathcal{H})$  is spanned by a set of  $N^2$  orthogonal density operators.

**Proposition 1.** *For any Hilbert space  $\mathcal{H}$  with dimension  $N$  there is a basis of density operators  $B_D \subset D(\mathcal{H})$  with size  $N^2$  which spans the space of Hermitian operators  $H(\mathcal{H})$ .*

*Proof.* Let's consider a set of vectors spanning the space  $\mathcal{H}$ :

$$\{|u_i\rangle : u_i[j] = \delta_{ij}, i \in [N], j \in [N]\}$$

We will define the basis set  $B_H$  of Hermitian operators as follows:

$$B_H = \{b^{ii} : i \in [N]\} \cup \\ \{b^{ij} + b^{ji} : 1 \leq i < j \leq N\} \cup \\ \{i(b^{ij} - b^{ji}) : 1 \leq i < j \leq N\},$$

where  $b^{ij}$  are Hermitian operators:

$$b^{ij} = |u_i\rangle \langle u_j|, 1 \leq i \leq j \leq N,$$

and  $i$  is the imaginary unit. It is easy to verify that the set  $B_H$  contains  $N^2 = N + \binom{N}{2} + \binom{N}{2}$  linearly independent operators which span the space  $H(\mathcal{H})$ . We will define a basis of density operators  $B_D$  which span  $H(\mathcal{H})$  by transforming the elements of  $B_H$  (which are not density operators) to density operators using operation of element-wise summation and scalar multiplication. These operations will change the Hermitian basis  $B_H$  to a density basis  $B_D$  as follows:

- The set of diagonal operators  $b^{ii}$  which are density operators will not be changed.
- The non-diagonal operators  $b^{ij} \pm b^{ji}$  are traceless and we will add 1-s to the diagonal elements corresponding to the non-zero (unit) off diagonal elements. In order to normalize the trace we multiply the operators by  $\frac{1}{2}$ .

The basis set of density operators then becomes:

$$\begin{aligned}
B_D = & \{b^{ii} : i \in [N]\} \cup \\
& \{b^{ij} + b^{ji} + \frac{1}{2}(b^{ii} + b^{jj}) : 1 \leq i < j \leq N\} \cup \\
& \{i(b^{ij} - b^{ji}) + \frac{1}{2}(b^{ii} + b^{jj}) : 1 \leq i < j \leq N\}.
\end{aligned} \tag{41}$$

This set is linearly independent and spans  $H(\mathcal{H})$  since it is a transformation of the base set  $B_H$  by real scalar multiplication and summation of base's elements  $\square$

The existence of a set of orthogonal density operators with size  $N^2$  that span the space  $H(\mathcal{H})$  allows to estimate an upper bound on the rank of the stochastic process languages described by QHMMs

**Theorem 2.** *For every classical HMM  $\mathbf{M}$  of order  $n$  there exists a QHMM  $\mathbf{Q}$  of order  $N = \sqrt{n}$  which generates the same stochastic language.*

*Proof.* Let  $\mathbf{M}$  be any classical HMM as described in **Definition 1**. The set of observable operators  $\mathbf{T} = \{T_a | a \in \Sigma\}$  (4) defines a stochastic process language  $L^M$  (9). In any moment of time the classical system is in superposition of its states described by a stochastic vector

$$\mathbf{x} = [p_1 \dots p_n],$$

where  $p_i$  is the probability of the classical state  $s_i$ . If the system undergoes evolution (4) and a symbol  $a$  is emitted the new state distribution is

$$\mathbf{x}' = T_a \mathbf{x}, \tag{42}$$

where the new classical states probabilities are

$$p'_i = \sum_{j=1}^n T_{a,ij} p_j, i = 1, \dots, n. \tag{43}$$

Consider a quantum system  $\mathbf{Q}$  (as defined in **Definition 2**) within a Hilbert space of dimension  $N = \sqrt{n}$ . By **Proposition 1**, there exists a basis of density operators  $\{b_i\}_{i=1}^n$  that spans the space of Hermitian operators  $H(\mathcal{H})$ . We map each classical state  $s_i$  to the density operator  $b_i$ . The classical stochastic state  $\mathbf{x}$  corresponds to the density operator

$$\rho_x = \sum_{i=1}^n p_i b_i \tag{44}$$

For every observable symbol  $a \in \Sigma$  we define quantum operation  $\mathcal{K}_a$  acting on the state  $\rho_x$  :

$$\mathcal{K}_a \rho_x = \sum_{ij} K_{a,ij} \rho_x \sum_{ij} K_{a,ij}^\dagger \tag{45}$$

where

$$K_{a,ij} = \sqrt{T_{a,ij}} b_i^{\frac{1}{2}} b_j^{\frac{1}{2}} \tag{46}$$

and  $b_i^{\frac{1}{2}}$  is the matrix square root of  $b_i$ .

Applying the operation  $\mathcal{K}_a$  to the state  $\rho_x$  results in a state

$$\rho_{x'} = \mathcal{K}_a \rho_x, \tag{47}$$

which can be presented in the basis  $\{b_i\}_{i=1}^n$  as

$$\rho_{x'} = \sum_{i=1}^n p'_i b_i. \tag{48}$$

We transform (47) using the operator-sum representation (45) of  $\mathcal{K}_a$  and (44):

$$\begin{aligned}
\rho_{x'} &= \sum_{ij} K_{a,ij} \left( \sum_{k=1}^n p_k b_k \right) \sum_{ij} K_{a,ij}^\dagger \\
&= \sum_{ij=1}^n \sum_{k=1}^n p_k K_{a,ij} b_k K_{a,ij}^\dagger.
\end{aligned} \tag{49}$$

Since  $b_i$  are orthogonal matrices using (46) we can simplify (49):

$$\begin{aligned}
\rho_{x'} &= \sum_{ij=1}^n p_j T_{a,ij} b_i \\
&= \sum_{i=1}^n \left( \sum_{j=1}^n T_{a,ij} p_j \right) b_i \\
&= \sum_{i=1}^n p''_i b_i,
\end{aligned} \tag{50}$$

where the probability of the quantum states  $b_i$  are

$$p''_i = \sum_{j=1}^n T_{a,ij} p_j, i = 1, \dots, n \tag{51}$$

The equivalence between the classical distribution (43) and the quantum distribution (51), resulting from the action of classical observable operators and their corresponding quantum operations, demonstrates that, given identical initial distributions, both models will generate the same stochastic process language.  $\square$

### III.A. Unitary Definition of QHMM

The definition of a QHMM in the previous section is based on the concept of a POVM operation acting on a quantum state. The emission of the observable symbols is encoded in the operational elements

(Kraus operators) of the quantum operation. This framework provides a convenient way to view QHMMs as channels for quantum information processing. It allows for the analysis of their informational complexity, expressive capacity, and establishes connections to stochastic process languages and the corresponding automata. However, this approach cannot be directly used for implementation of the QHMMs on quantum computing hardware.

In Section II B we demonstrated that every POVM operation  $\mathcal{T}$  defined in Hilbert space  $\mathcal{H}_S$  can be represented as composition of basic quantum operations:

1. Dilation of the “state” system with an “emission” quantum system  $\mathcal{H}_E$ :

$$\mathcal{H}_S \mapsto \mathcal{H}_S \otimes \mathcal{H}_E.$$

2. Unitary transformation  $U$ , entangling the components of the bipartite system  $\rho_{SE}$ :

$$U(\rho_S \otimes \rho_E)U^\dagger.$$

3. Partial trace over the emission component, which provides the reduced density of the state system as the output of the operation:

$$\rho_S = \text{tr}_E (U(\rho_S \otimes \rho_E)U^\dagger).$$

The minimal dimension of the emission system  $\mathcal{H}_E$  corresponds to the Kraus rank of the operation  $\mathcal{T}$ . This rank quantifies the operation’s complexity by indicating the minimal auxiliary resources required for its unitary implementation. The unitary implementation of a QHMM relies on Stinespring’s dilation theorem [39], which states that any quantum operation can be represented as a unitary evolution on a larger (dilated) system.

**Theorem 3.** Any QHMM  $\mathbf{Q} = \{\Sigma, \mathcal{H}_S, \mathcal{T} = \{T_a\}_{a \in \Sigma}, \rho_0\}$  has parameterization in terms of a unitary  $U$  defined in a dilated Hilbert space  $\mathcal{H}$ , where  $\dim \mathcal{H} \geq \dim \mathcal{H}_S + |\Sigma|$ .

*Proof.* Let’s introduce an auxiliary (“emission”) quantum system with Hilbert space  $\mathcal{H}_E$ ,  $\dim(\mathcal{H}_E) = M$ ,  $M = |\Sigma|$ , and orthonormal basis  $\{|e_i\rangle\}_{i=0}^{M-1}$ . We assume that  $\text{ord}(a)$  is the position of the symbol  $a$  in the set  $\Sigma = \{a_1, \dots, a_{M-1}\}$ . Let’s select a specific state  $|e_0\rangle$  to be the initial state. A linear operator  $V : \mathcal{H}_S \rightarrow \mathcal{H}_S \otimes \mathcal{H}_E$  is defined as follows:

$$V : |v\rangle \mapsto \sum_{a \in \Sigma} T_a |v\rangle \otimes |e_{\text{ord}(a)}\rangle, |v\rangle \in \mathcal{H}_S. \quad (52)$$

Since the quantum operation  $\mathcal{T}$  is complete:  $\sum_{a \in \Sigma} T_a^\dagger T_a = I_N$ , the operator  $V$  is an isometry:

$V^\dagger V = I_N$ , and it can be extended to a unitary operator  $U : \mathcal{H}_S \otimes \mathcal{H}_E \rightarrow \mathcal{H}_S \otimes \mathcal{H}_E$  by using the Gram-Schmidt process [24].

If we apply the unitary operator  $U$  to the dilated system  $\mathcal{H}_S \otimes \mathcal{H}_E$  and trace over the emission subsystem

$$\text{tr}_E (U(|v\rangle \langle v| \otimes |e_0\rangle \langle e_0|)U^\dagger) = \sum_{a \in \Sigma} T_a |v\rangle \langle v| T_a^\dagger,$$

where  $|v\rangle \in \mathcal{H}_S$ , we derive the operator-sum representation of  $\mathbf{Q}$ . Hence, the unitary  $U$  parameterizes the QHMM.  $\square$

The above parameterization is unique up to unitary transformation on the selected basis of the emission system.

Every unitary operator  $U$  acting on a composite system  $\mathcal{H}_{SE} = \mathcal{H}_S \otimes \mathcal{H}_E$  defines a quantum operation by the Kraus operators (31). Every quantum operation defines a unitary operator on a dilated system through the isometry  $V$  (52). This equivalence allows us to provide a formal definition of unitary QHMMs.

**Definition 3** (Unitary Quantum Hidden Markov Model). A Unitary Quantum HMM  $\mathbf{Q}$  over an alphabet of observable symbols  $\Sigma$  and finite  $N$ -dimensional Hilbert space is a 6-tuple:

$$\mathbf{Q} = \{\Sigma, \mathcal{H}_S, \mathcal{H}_E, U, \mathcal{M}, R_0\}$$

where

- $\Sigma$  is a finite set of  $m$  observable symbols.
- $\mathcal{H}_S$  is the Hilbert space of the hidden state system of dimension  $N$ .
- $\mathcal{H}_E$  is the Hilbert space of an auxiliary emission system with dimension  $m \leq M \leq N^2$  and orthonormal basis  $E = \{|e_i\rangle\}_{i=0}^{M-1}$ .
- $U$  is a unitary operator defined on the bipartite Hilbert space  $\mathcal{H}_S \otimes \mathcal{H}_E$ .
- $\mathcal{M}$  is a bijective map  $\mathcal{P}_m^E \rightarrow \Sigma$ , where  $\mathcal{P}_m^E$  is an  $m$ -element partition of  $E$ .
- $R_0 = \rho_0 \otimes |e_0\rangle \langle e_0|$  is an initial state.

The Algorithm 1 simulates a unitary QHMM  $\mathbf{Q}$  for  $T$  steps and generates a sequence of the process language  $L^{\mathbf{Q}}$ . The same generation process is presented graphically on FIG 2.

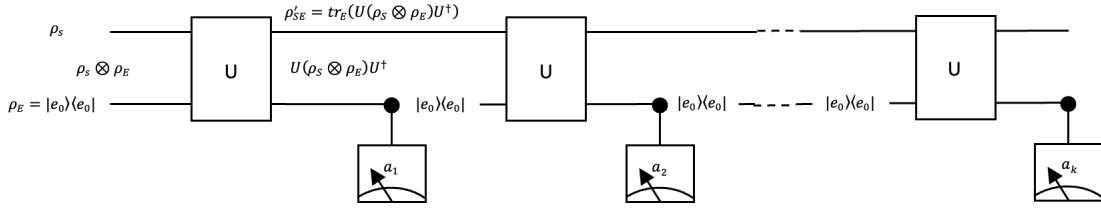


FIG. 2. Unitary Simulation of a Quantum Operation.

**Algorithm 1: QHMM Unitary Simulation****Input :** QHMM

$$\mathbf{Q} = \{\Sigma, \mathcal{H}_S, \mathcal{H}_E, U, \mathcal{M}, R_0 = \rho_0 \otimes |e_0\rangle\langle e_0|\}$$

**Output:** Generated Sequence  $\mathbf{a}$ **1 Initialize:**

- **State system**  
 $\mathcal{H}_S, \dim(\mathcal{H}_S) = N, \rho_S = \rho_0$
- **Emission system**  $\mathcal{H}_E, \dim(\mathcal{H}_E) = M, m \leq M \leq N^2, \rho_E = |e_0\rangle\langle e_0|$
- **Prepare product state**  
 $\rho_{SE} = \rho_S \otimes \rho_E$
- **Sequence length:**  $T$
- **Current Step:**  $t \leftarrow 0$
- **Output Sequence:**  $\mathbf{a} \leftarrow \epsilon$

**2 while**  $t \leq T$  **do**

```

3    $\rho_{SE} \leftarrow U\rho_{SE}U^\dagger$  /* Apply unitary on
   full system */
4    $\rho_S \leftarrow \text{tr}_E(\rho_{SE})$  /* Projective
   measurement of  $\rho_E$  */
5    $o \leftarrow e_i$  /* Measurement outcome  $o$  */
6    $\mathbf{a} \leftarrow \mathbf{a} + \mathcal{M}(E_o), E_o \in \mathcal{P}_m^E, o \in E_o$ 
   /* Emit symbol for outcome  $o$  */
7    $\rho_{SE} \leftarrow \rho_S \otimes |e_0\rangle\langle e_0|$  /* Set  $\rho_E$  to
   initial state */
8    $t \leftarrow t + 1$ 

```

**9 return**  $\mathbf{a}$ 

**Example 2.** In [25], Monras et al. discuss an example of QHMM in Hilbert space with dimension 2, which defines a stochastic process language with Hankel matrix of rank 3. This is an example where the minimal classic HMM (of order 3) is more complex than the equivalent QHMM. The quantum model  $\mathbf{Q}$  is defined as follows:

$$\mathbf{Q} = \{\Sigma, \mathcal{H}_S, \mathcal{T} = \{\mathcal{T} = \{T_a\}_{a \in \Sigma}, \rho_0\},$$

where

- $\Sigma = \{0, 1, 2, 3\}$  is an alphabet of observable symbols.
- $\mathcal{H}_S$  is a Hilbert space with dimension 2 (i.e.  $\mathbf{Q}$  is a 1 qubit quantum system).
- The operator-sum representation of  $\mathcal{T}$  is  $\mathcal{T}_a = K_a \cdot K_a^\dagger$ , where the Kraus operators are:  $K_0 = \frac{1}{\sqrt{2}} |\uparrow\rangle\langle\uparrow|$ ,  $K_1 = \frac{1}{\sqrt{2}} |\downarrow\rangle\langle\downarrow|$ ,  $K_2 = \frac{1}{\sqrt{2}} |+\rangle\langle+|$ , and  $K_3 = \frac{1}{\sqrt{2}} |-\rangle\langle-|$ .
- $\rho_0$  is the maximally entangled initial state.

We provide the following unitary definition of the same QHMM:

$$\mathbf{Q} = \{\Sigma, \mathcal{H}_S, \mathcal{H}_E, U, \mathcal{M}, \rho_0 \otimes |e_0\rangle\langle e_0|\},$$

where

- $\Sigma = \{0, 1, 2, 3\}$ .
- $\mathcal{H}_S$  is the state system Hilbert space with dimension 2.
- $\mathcal{H}_E$  is the emission Hilbert space with dimension 4 (i.e. a 2 qubit quantum system with a measurement basis  $\{|e\rangle \in [0, 1, 2, 3]\}$ ), corresponding to the observable symbols.
- $U$  is the unitary operation implemented by the “State transition” circuit in FIG 3.
- $\rho_0$  is the maximally mixed state implemented by the “Max mixed state” circuit in FIG 3.
- $\mathcal{M}$  is the identity  $\{0, 1, 2, 3\} \rightarrow \{0, 1, 2, 3\}$ .

The circuit generating sequences with length 2 and their distribution are shown in FIG 3 and FIG 4. The “X” gates controlled on the classical “observable” registers  $o_0$  and  $o_1$  are used to reset the emission system to the initial state  $|e_0\rangle$ .

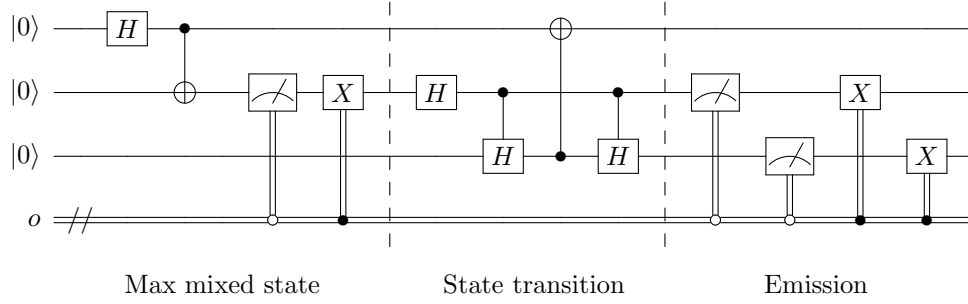


FIG. 3. QHMM generating 1-symbol sequences, Monras et al. [25]

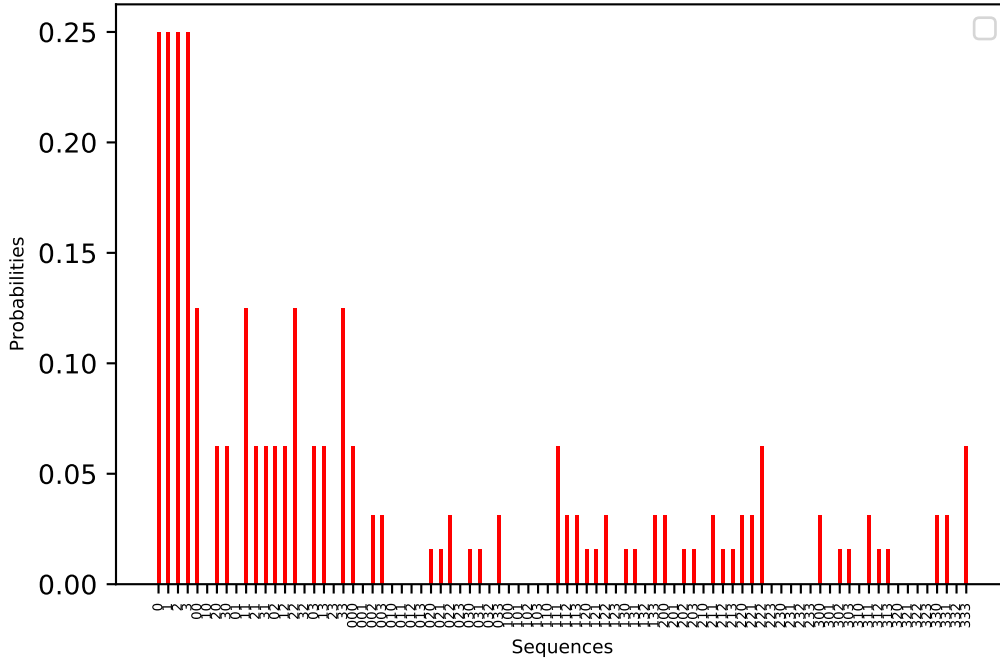


FIG. 4. Observable Sequences Distribution, Monras et al. [25]

### III.B. Primary and Measurement System Design. Test Case for the Circuit Ansatz Design

To get ideas for system design we refer to the theory of open quantum systems, which studies the system dynamics under the system-environment interaction [50]. Researchers consider Markovian and non-Markovian time evolutions [51, 52]. The precise definition of (non-) Markovianity is a subject of ongoing research [53, 54]. The major difference between these two evolution regimes are the

memory effects in the non-Markovian case. Non-Markovian regime complicates the dynamics of the system, makes it irreversible, e.g. see [55]. The information in non-Markovian evolution flows from the system to the environment and from the environment to the system [56]. In real physical systems the description of the environment or even its dimension may not be known to us, however, in the present research we design both the system and the environment to model stochastic processes, so we have full control.



Building on the inspiration from the open quantum systems we consider two circuit designs to implement QHMM (FIG 5).

The circuit on FIG 5 a) collapses the state of the environment to the ground state after the first iteration of the unitary evolution with  $U_{AE}$ . The state of the system collapses to the result of the measurement so it is the only information transmitted to the next iteration. The circuit on FIG 5 b) may exhibit longer term memory effects.

For circuit training purposes we introduce a separate transformation of the measurement system  $U_{Meas}$  (FIG 6):

$$U_{AE} = (U_{Meas} \otimes I)U_{AE}^1$$

The choice of the initial state depends on the use case. In the examples shown on FIG 25 and FIG 27 below we use maximally mixed state as the initial state.

Based on the preliminaries in Section II B we can write the probability of a sequence for the circuit FIG 5 a) as

$$\Pr\{j_1 j_2 \dots j_k\} = \text{Tr} \left\{ M_{j_k} \sum_i K_i \dots M_{j_2} \sum_i K_i M_{j_1} \sum_i K_i \rho_A K_i^\dagger M_{j_1}^\dagger K_i^\dagger M_{j_2}^\dagger \dots K_i^\dagger M_{j_k}^\dagger \right\} \quad (53)$$

where  $M$  are projective measurements, and  $K$  are Kraus operators  $K_i = (I \otimes \langle e_i |) U (I \otimes |e_0\rangle)$ . Please, note that the same expression for the circuit FIG 5 b) would be much more complicated, since the start state  $e_0$  of the environment may be changing between iterations creating a new set of Kraus operators each time.

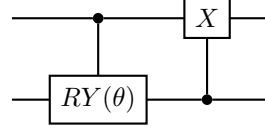
How do we know that the circuit on FIG 5 a) is able to produce probabilities according to the equation EQ 53? Here we suggest to use a well-known quantum operation - amplitude damping noise model [24, 57] as a test case and build a sequence generator. It is described by the following unitary transformation:

$$U_{AD} = \begin{pmatrix} 1 & 0 & 0 & 0 \\ 0 & 0 & 0 & 1 \\ 0 & -\sqrt{\gamma} & \sqrt{1-\gamma} & 0 \\ 0 & \sqrt{1-\gamma} & \sqrt{\gamma} & 0 \end{pmatrix},$$

which, alternatively, can be represented in a circuit form:

$$U_{AD} = (I \otimes |0\rangle\langle 0| + X \otimes |1\rangle\langle 1|) \times (|0\rangle\langle 0| \otimes I + |1\rangle\langle 1| \otimes RY(\theta))$$

or



where  $\gamma = \sin^2(\frac{\theta}{2})$ . The full circuit is shown on FIG 7.

From this unitary we derive Kraus operators describing evolution of the principal subsystem given that the start state of the environment is  $e_0 = |0\rangle$ :

$$\begin{aligned} \mathbf{K}_0 &= \left( \begin{pmatrix} 1 \\ 0 \end{pmatrix} \otimes \begin{pmatrix} 1 & 0 \\ 0 & 1 \end{pmatrix} \right)^\dagger U \left( \begin{pmatrix} 1 \\ 0 \end{pmatrix} \otimes \begin{pmatrix} 1 & 0 \\ 0 & 1 \end{pmatrix} \right) \\ &= \begin{pmatrix} 1 & 0 \\ 0 & 0 \end{pmatrix}, \end{aligned}$$

$$\begin{aligned} \mathbf{K}_1 &= \left( \begin{pmatrix} 0 \\ 1 \end{pmatrix} \otimes \begin{pmatrix} 1 & 0 \\ 0 & 1 \end{pmatrix} \right)^\dagger U \left( \begin{pmatrix} 1 \\ 0 \end{pmatrix} \otimes \begin{pmatrix} 1 & 0 \\ 0 & 1 \end{pmatrix} \right) \\ &= \begin{pmatrix} 0 & -\sqrt{\gamma} \\ 0 & \sqrt{1-\gamma} \end{pmatrix}. \end{aligned}$$

In this test case we want to compare the sequence probabilities calculated using EQ 53 with circuit (FIG 7) results, when it is run on the simulator and on *ibmq\_montreal* hardware device. The probabilities calculated on the simulator will include shot, or sampling, noise. In order to reduce this error we use 100,000 shots. The hardware result will include both: hardware and shot noise. The circuit that was run on the simulator and *ibmq\_montreal* hardware device is shown on FIG 8. Please note that the measurements are recorded on the classical register in reverse order following Qiskit's convention of putting the least significant bit to the right. Mid-circuit measurement and reset instructions have become available fairly recently in early 2021 [58]. They are now part of a broader dynamic circuit capability introduced in 2022 [59].

The comparison of the sequence probabilities is shown on FIG 9.

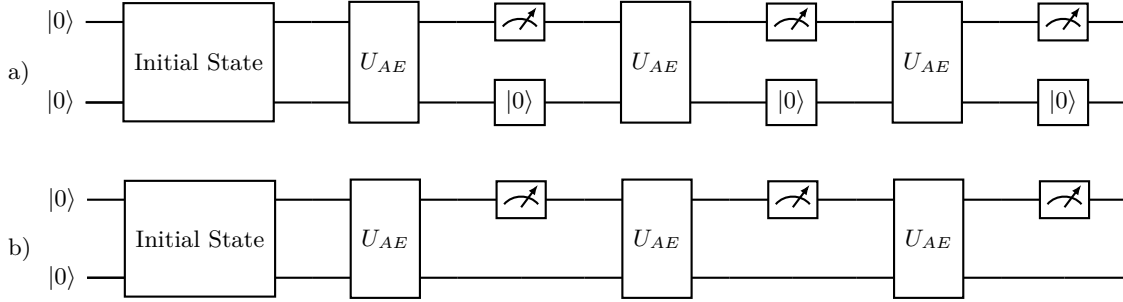


FIG. 5. QHMM Circuit Ansatz Design

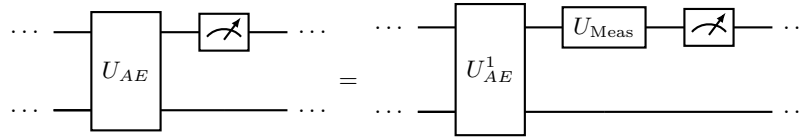


FIG. 6. Separated Measurement System Transformation

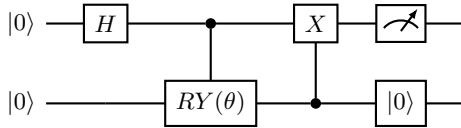


FIG. 7. Amplitude damping test case circuit for 1 step sequence

All calculations produce identical results up to sampling and hardware errors, so we confirm that our approach works as expected. It is worth noting that hardware results are very close to simulations. Here we have used *Sampler* primitive in *Qiskit Runtime* to run this experiment [60]. Behind the scenes this primitive implements error mitigation [61]. We have repeated the experiments for a range of  $\gamma$  parameters including the edges 0 and 1. In all cases, we observed the same level of agreement between the results.

The Hankel matrix for the current process is shown in Table II. The rank of the Hankel matrix changes with the length of the sequence (see FIG 10). It is interesting to note that if we choose a different start state on the quantum circuit - use excited state  $|1\rangle$  instead of  $|+\rangle$  state, then the Hankel matrix will have rank 2 for all sequences of length 2 and above.

#### IV. LEARNING QUANTUM HIDDEN MARKOV MODELS

In this section, we formalize and study the problem of learning QHMMs. The learning problem is defined as follows: given an empirical specification of a stochastic process language  $L$ , which is referred to as the learning target, the objective is to find a QHMM  $Q$  that is equivalent or approximates the sequence function  $f^L$  of the target. We discuss and formalize the components of the learning problem which include:

- Specification of the target stochastic language by estimating of its characteristics from the data. These characteristics may include order, Hankel matrix, finite distributions.
- Definition of a set of potential solutions or a hypotheses space of unitary QHMMs.
- Design of hypotheses' quality criteria or a fitness function.
- Design of learning algorithms.

##### IV.A. Empirical Specification of Stochastic Languages

For every stochastic process language  $L$  we defined a sequence function  $f^L$  and corresponding generalized Hankel matrix  $H^L$  (9). Sequence function  $f^Q$

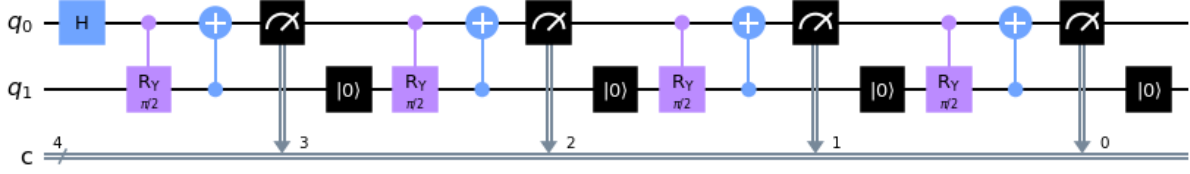


FIG. 8. Amplitude damping noise circuit in Qiskit.  $\theta = \frac{\pi}{2}$

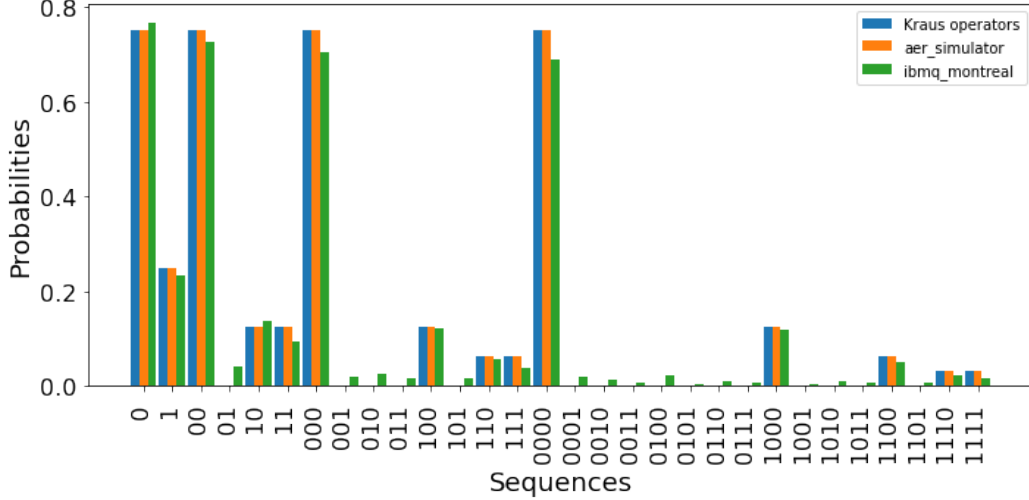


FIG. 9. Sequence probabilities for amplitude damping noise model.  $\theta = \frac{\pi}{2}$

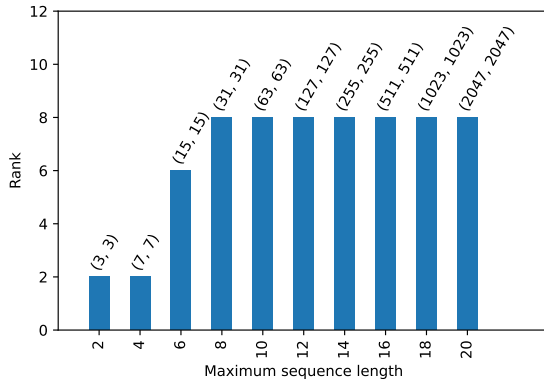


FIG. 10. Hankel matrix rank for different length sequences. Hankel matrix dimensions are shown in parentheses.

and Hankel matrix  $H^Q$  are defined for the language of every QHMM  $Q$  as well (36), (37). We assume that the target stochastic language is specified by a finite sample of the functional relation  $f^L$ , respectively a finite sub-matrix of  $H^L$ . If the sample is

derived analytically or through exhaustive simulation of a known HMM, then its probabilities will be exactly the same as the probabilities of the target distribution. It is possible though, that the sample is derived through observation of a "natural" random source which is assumed to be Markovian. In this case the probabilities of the sample need to be estimated and this will have impact on the precision of the learned model. First, we discuss the size of a "representative" sample for a language or the *sample complexity* of the learning problem. It is known [42] that if a language  $L$  is defined by a classic HMM of order  $n$  then it is uniquely specified by the probabilities of all sequences up to length  $2n - 1$ . If the alphabet  $\Sigma$  contains  $m$  symbols this estimate defines a sample size of  $\sum_{i=1}^{2n-1} m^i$  probabilities. If it is acceptable the specification to be valid for *almost all* HMMs-defined languages excluding a set with measure zero [44], then the representative sample would contain the probabilities of all sequences of length exactly  $2l + 1$  where  $l > 8 \lceil \log_m n \rceil$  or  $m^{2l+1}$  probabilities. In many learning scenarios, a classical HMM for the learning target is not provided, and in some cases, it is not known whether such an HMM exists.

	empty	0	1	00	01	10	11
empty	1	0.75	0.25	0.75	0	0.125	0.125
0	0.75	0.75	0	0.75	0	0	0
1	0.25	0.125	0.125	0.125	0	0.0625	0.0625
00	0.75	0.75	0	0.75	0	0	0
01	0	0	0	0	0	0	0
10	0.125	0.125	0	0.125	0	0	0
11	0.125	0.0625	0.0625	0.0625	0	0.03125	0.03125

TABLE II. Hankel matrix of the amplitude damping process.

Instead, the only available training data consists of a set of observed sequences, each of length  $T$ , sampled from an unknown process language  $L$ :

$$\mathcal{Y}^L = \{\mathbf{y}_1, \dots, \mathbf{y}_T : \mathbf{y}_i \in \Sigma^T\}.$$

Using these empirical samples we have to estimate the sequence function (9) and then the order and the finite distributions of the unknown language. To estimate the sequence function for sequences with length  $k$  we construct the following set:

$$\mathbf{S}_k = \{\mathbf{a} : |\mathbf{a}| = k, \exists \mathbf{p}, \mathbf{s} \in \Sigma^*, \exists y \in \mathcal{Y}_L : \mathbf{pas} = \mathbf{y}\}. \quad (54)$$

If the sample  $\mathbf{S}_k$  contains  $m$  independently drawn sequences from the unknown distribution  $D_k^L$ , then the estimate  $\hat{f}(\mathbf{a})$  is the empirical frequency of  $\mathbf{a}$  in  $\mathbf{S}_k$ :

$$\hat{f}(\mathbf{a}) = \frac{1}{m} \sum_{\mathbf{b} \in \mathbf{S}_k} \mathbf{1}_{\mathbf{a}}(\mathbf{b}).$$

The estimate of the finite distributions  $D_k^L$  is

$$\hat{D}_k^L = \{\hat{f}(\mathbf{a}) : \mathbf{a} \in \mathbf{S}_k\} \quad (55)$$

The approximation of the Hankel matrix is:

$$\hat{H}[\mathbf{u}, \mathbf{v}] = \hat{f}(\mathbf{uv}), |\mathbf{uv}| = k.$$

The error of this approximation depends on the sample size  $m$  [62] and is restricted as follows:

$$\|H - \hat{H}\| \leq \mathcal{O}\left(\frac{1}{\sqrt{m}}\right).$$

If we are given a sample  $\mathcal{Y}^L$  with no additional information we have to estimate a plausible order of the classical model by the maximum rank of the Hankel matrix. We start with low sequences length and estimate the rank increasing the length. If at particular sequence length the rank does not increase anymore we can use this rank as an estimate. This procedure will provide only local approximation since the problem to infer the rank of the Hankel matrix from data is undecidable [46].

#### IV.B. QHMM Hypotheses Space

The hypotheses space  $\mathbb{Q}$  of the learning problem contains the unitary QHMMs (**Definition 3**):

$$\mathbb{Q} = \{\mathbf{Q} : \mathbf{Q} = (\Sigma, \mathcal{H}_S, \mathcal{H}_E, U, \mathcal{M}, \rho_0)\}, \quad (56)$$

where the parameters are specified and restricted by the given samples of the target stochastic process language:

- The alphabet  $\Sigma$  contains the observed  $m$  symbols.
- $\mathcal{H}_S$  is a Hilbert space with dimension  $\hat{N} = \lceil \sqrt{\hat{r}} \rceil$  where  $\hat{r}$  is the estimated maximal rank of the Hankel matrix built for the data sample  $\mathcal{Y}$ .
- $\mathcal{H}_E$  is a Hilbert space with dimension  $2^{\lceil \log_2 m \rceil} \leq M \leq \hat{N}^2$ . We select any orthonormal basis  $\mathcal{E} = \{|e_0\rangle \dots |e_{M-1}\rangle\}$  of  $\mathcal{H}_E$ .
- $U$  is a unitary operation on the Hilbert space  $\mathcal{H}_S \otimes \mathcal{H}_E$  implemented by a quantum circuit of  $\log_2 \hat{N} + \log_2 M$  qubits using gates from a base gates type set  $\mathcal{G} = \{g_0 \dots g_k\}$ .
- $\mathcal{M}$  is a bijective map  $\mathcal{P}_m^E \rightarrow \Sigma$ , where  $\mathcal{P}_m^E$  is an  $m$ -element partition of  $E$ .
- $\rho_0$  is initial state implemented as one of the following: the maximally entangled state, the maximally mixed state, or the ground state.

Every hypothesis  $\mathbf{Q}$  defines a sequence function  $f^{\mathbf{Q}}$  and corresponding Hankel matrix  $H^{\mathbf{Q}}$  which are used for evaluation of its quality. Every unitary operator  $U$  has representation as a quantum circuit  $\mathcal{C}_U$  with linear structure

$$\mathcal{C}_U = (g_i)_{i \geq 1}. \quad (57)$$

The quantum gates  $g_i$  are encoded as 3-tuples:

$$g = \langle \mathbf{t}, ([q_c, ]q_d), ([p_1[, p_2]]) \rangle \quad (58)$$

where  $\mathbf{t} \in \mathcal{G}$  is the gate's type,  $q_c$  and  $q_d$  are the control and data qubits, and  $p_1, p_2$  are gate's parameters. We will make the assumption that the set of gate types  $\mathcal{G}$  includes single-qubit gates and two-qubit controlled gates.

Formally, the hypothesis space is the infinite set of all finite quantum circuits in the  $NM$ -dimensional Hilbert space  $\mathcal{H}_S \otimes \mathcal{H}_E$ , encoded as lists of gates (58).

### IV.C. Quality of a Hypothesis

#### IV.C.1. Precision of a Hypothesis

A standard measure of the quality of a generative hypothesis  $Q$  defining language  $L^Q$  is its variational distance to the target distributions  $D^L(2)$ . Let's assume that the distributions  $D^L$  are defined by an unknown target QHMM model. The divergence between the target and the hypothesis for any sequence  $\mathbf{a} \in \Sigma^*$  can be defined as the divergence in probabilities assigned to the sequence  $\mathbf{a}$  by the target and the hypothesis(35):

$$\begin{aligned} \delta^{LQ}(\mathbf{a}) &= |P[\mathbf{a}|L] - P[\mathbf{a}|Q]| \\ &= |\text{tr}(T_{\mathbf{a}}^L \rho_0) - \text{tr}(T_{\mathbf{a}}^Q \rho_0)| \\ &= |\text{tr} \rho_{\mathbf{a}}^L - \text{tr} \rho_{\mathbf{a}}^Q|, \end{aligned} \quad (59)$$

where  $\mathcal{T}^L = \{T_{\mathbf{a}}^L\}_{\mathbf{a} \in \Sigma}$  and  $\mathcal{T}^Q = \{T_{\mathbf{a}}^Q\}_{\mathbf{a} \in \Sigma}$  are the quantum operations of the target model and the hypothesis and we assume a fixed initial state  $\rho_0$ . The quantum states  $\rho_{\mathbf{a}}^L = T_{\mathbf{a}}^L \rho_0$  and  $\rho_{\mathbf{a}}^Q = T_{\mathbf{a}}^Q \rho_0$  represent the sequence generation paths under the target and the hypothesis models. The usual measurable distance between two quantum states is the *trace norm*  $\|\rho_{\mathbf{a}}^L - \rho_{\mathbf{a}}^Q\|_1 = \text{tr} |\rho_{\mathbf{a}}^L - \rho_{\mathbf{a}}^Q|$ . In the context of learning a QHMM, it is not feasible to directly measure the trace norm because the target model is generally unknown or may not even exist. The introduced divergence  $\delta^{LQ}$  can be estimated empirically and is dominated by the theoretical trace norm:

$$\begin{aligned} \delta^{LQ}(\mathbf{a}) &= |\text{tr} \rho_{\mathbf{a}}^L - \text{tr} \rho_{\mathbf{a}}^Q| \\ &= \left| \sum_{i=1}^N (\rho_{\mathbf{a}}^L)_{ii} - (\rho_{\mathbf{a}}^Q)_{ii} \right| \\ &\leq \sum_{i=1}^N |(\rho_{\mathbf{a}}^L)_{ii} - (\rho_{\mathbf{a}}^Q)_{ii}| \\ &= \text{tr} |\rho_{\mathbf{a}}^L - \rho_{\mathbf{a}}^Q|. \end{aligned} \quad (60)$$

This relation will be used later in our analysis of QHMMs learning difficulty.

The divergence between the target language and the hypothesis on finite distributions of sequences with lengths exactly  $n$  is

$$\Delta_n(D^L || D^Q) = \max_{\mathbf{a} \in \Sigma^n} \delta^{LQ}(\mathbf{a}) \quad (61)$$

The average divergence between the hypothesis  $Q$  and the target  $L$  when given finite sample of sequences with lengths up to  $n$  is defined as

$$\Delta_{\leq n}(D^L || D^Q) = \frac{1}{n} \sum_{i=1}^n \Delta_i(D^L || D^Q) \quad (62)$$

We will refer to the average divergence (62)  $\Delta_{\leq n}(D^L || D^Q)$  as the *empirical divergence* between a hypothesis and the learning target.

The *empirical divergence rate* of the hypothesis  $Q$  with respect to the target  $L$  is defined as

$$\hat{\Delta}(D^L || D^Q) = \lim_{n \rightarrow \infty} \Delta_{\leq n}(D^L || D^Q), \quad (63)$$

if the limit exists and it is finite.

We can prove that the empirical divergence rate between any QHMM hypothesis and a finite order stochastic process language converges with the increase of the sequences length  $n$  of the finite distributions in the learning sample.

**Proposition 2.** *If the learning target  $L$  is a finite order stochastic process language, then for any hypothesis  $Q \in \mathcal{Q}$  the empirical divergence rate (63)*

$$\hat{\Delta}(D^L || D^Q) = \lim_{n \rightarrow \infty} \Delta_{\leq n}(D^L || D^Q)$$

*exists and is finite.*

*Proof.* For the finite order process languages the estimate of the relative entropy is consistent [63]:

$$\hat{D}_{KL}(D^L || D^Q) = \lim_{n \rightarrow \infty} \frac{1}{n} D_{KL}^n(D^L || D^Q) \quad (64)$$

where

$$D_{KL}^n(D^L || D^Q) = \sum_{\mathbf{a} \in \Sigma^n} P[\mathbf{a}|L] \log \frac{P[\mathbf{a}|L]}{P[\mathbf{a}|Q]}, \quad (65)$$

and the trace distance between the finite distributions is bounded by the relative entropy according to the Pinsker inequality:

$$D_{KL}(D^L || D^Q) \geq \frac{1}{2} D_{\text{tr}}^2(D^L || D^Q),$$

where

$$D_{\text{tr}}(D^L || D^Q) = \lim_{n \rightarrow \infty} D_{\text{tr}}(D_n^L || D_n^Q),$$

$$D_{\text{tr}}(D_n^L \| D_n^Q) = \frac{1}{n} \sum_{i=1}^n d_{\text{tr}}(D_i^L \| D_i^Q),$$

$$d_{\text{tr}}(D_i^L \| D_i^Q) = \sum_{\mathbf{a} \in \Sigma^i} \text{tr} |\rho_{\mathbf{a}}^L - \rho_{\mathbf{a}}^Q|.$$

From the inequality in (60) follows

$$\begin{aligned} D_{KL}(D_L \| D_Q) &\geq \frac{1}{2} D_{\text{tr}}^2(D^L \| D^Q) \\ &\geq \frac{1}{2} \hat{\Delta}^2(D^L \| D^Q), \end{aligned} \quad (66)$$

and we can conclude that the limit (63) exists in the cases when the target  $L$  is a finite order stochastic process language.  $\square$

The empirical divergence rate (63) can be estimated from a sample of the target language and is considered to be the *precision* of a hypothesis  $Q$ . This measure can be used in any approximate QHMM learning model even for languages which are not generated by any hypothesis in the space  $\mathbb{Q}$ .

Theoretically the divergence between the target  $L$  and a hypothesis  $Q$  defined by quantum operations  $\mathcal{T}^L$  and  $\mathcal{T}^Q$  (**Definition 2**) is the maximum probability divergence for sequences of length exactly  $n, n > 0$  over all initial states  $\rho_0$  is the trace norm defined as:

$$\|(\mathcal{T}^L)^n - (\mathcal{T}^Q)^n\|_1 = \max_{\rho} \|(\mathcal{T}^L)^n \rho - (\mathcal{T}^Q)^n \rho\|_1 \quad (67)$$

To estimate the relation between the trace divergence and the empirical divergence we consider the quantum states which define distributions over the sequences with length  $n$ :

$$\rho_n^i = (\mathcal{T}^i)^n \rho_0, \rho_0 \in D(\mathcal{H}_S), i = \{L, Q\}, \quad (68)$$

where  $\rho_0$  is an initial state. The trace norm  $\|\rho_n^L - \rho_n^Q\|_1$  is bounded from below by the empirical divergence (61) of  $Q$  as follows:

$$\begin{aligned} \|\rho_n^L - \rho_n^Q\|_1 &= \|(\mathcal{T}^L)^n \rho_0 - (\mathcal{T}^Q)^n \rho_0\|_1 \\ &= \max_{\mathbf{a} \in \Sigma^n} \|T_{\mathbf{a}}^L \rho_0 - T_{\mathbf{a}}^Q \rho_0\|_1 \\ &= \max_{\mathbf{a} \in \Sigma^n} \text{tr} |\rho_{\mathbf{a}}^L - \rho_{\mathbf{a}}^Q| \\ &\geq \max_{\mathbf{a} \in \Sigma^n} \delta^{LQ}(\mathbf{a}) \\ &= \Delta_n(D^L \| D^Q) \end{aligned} \quad (69)$$

From the inequality (69) follows that, given finite sample of sequences with length  $n$ , the empirical divergence between the hypothesis  $Q$  and the target  $L$  (61) is a lower bound of the trace divergence (67):

$$\Delta_n(D^L \| D^Q) \leq \|(\mathcal{T}^L)^n - (\mathcal{T}^Q)^n\|_1 \quad (70)$$

This inequality will be used to demonstrate a critical feature of the heuristic search approach to the learning of QHMMs: small changes in the norms of the unitary hypotheses lead to small changes of their precision.

#### IV.C.2. Complexity of a Hypothesis

Another measure of quality is the hypothesis' complexity. If we assume that the state Hilbert space  $\mathcal{H}_S$  has fixed dimension  $N$ , where  $N = \text{rank}(\hat{H}_L)$ , then the free parameters of a hypothesis  $Q$  are the unitary  $U$  and the dimension of the emission component  $M$ . If for a unitary  $U$  we denote by  $c_2(U)$  the number of two qubit gates then as a simple measure of its gate complexity we use the function:

$$C_g(Q) = \frac{c_2(U)}{\binom{NM}{2}}$$

The complexity of the unitary implementation is related also to the dimension of the emission system  $\mathcal{H}_E, |\Sigma| \leq M \leq N^2$ . The following measure reflects the dimension-related complexity:

$$C_e(Q) = \frac{M}{N^2}$$

The full complexity of a hypothesis is estimated as follows:

$$C(Q) = c_q C_q(Q) + c_e C_e(Q), \quad (71)$$

where  $c_q$  and  $c_e$  are real hyper parameters reflecting the trade-off between complex unitary or wider circuit.

We will integrate the hypothesis' precision (62) and complexity (71) measures into a single quality function called *fitness* which is defined as follows:

$$F(Q) = -(D^n(D_L \| D_Q) + C(Q)), \quad (72)$$

#### IV.D. Formalization of the QHMM Learning Problem

We will discuss a specific formalization of the QHMM learning problem defined as follows:

**Definition 4** (Unitary QHMM learning problem). *A Unitary Quantum HMM learning problem is defined as follows. Given:*

- A sample  $\{D_t^L : 0 < t \leq n\}$  of the finite distributions of a unknown stochastic process language  $L$  (learning target),



- A unitary hypothesis space

$$\mathbb{Q} = \{Q : \mathbb{Q} = (\Sigma, \mathcal{H}_S, \mathcal{H}_E, U, \mathcal{M}, \rho_0)\}$$

defined in Section IV B,

- A fitness function  $F(Q)$  (72) defined over the hypothesis space,

find a hypothesis  $Q^* \in \mathbb{Q}$  that maximizes the fitness function:

$$Q^* = \operatorname{argmax}_{Q \in \mathbb{Q}} F(Q). \quad (73)$$

The corresponding classical HMM learning problem is expected to be computationally hard [64], therefore we propose the optimization task (73) to be approached by heuristic search algorithms.

The heuristic search algorithms use the fitness function as a heuristic search function, providing information about the distance and direction towards the optimal solution. Therefore the properties of the fitness function are strongly related to the complexity of the learning task. To examine this relationship, we utilize the concept of a *fitness landscape*, which represents a multidimensional surface defined as follows:

$$\{F(Q) : Q \in \mathbb{Q}\}. \quad (74)$$

Intuitively, an optimization task is expected to be efficient, if the points on the fitness landscape are correlated with the optimal point or at least with the points in their neighbourhoods. This property requires the landscape to be *smooth* and any small change of a hypothesis  $Q$  results in restricted change of its fitness function. To formalize these intuitive notions, we introduce appropriate metrics in the hypothesis spaces  $\mathbb{Q}$  and in the fitness space.

The distance in the hypothesis space is quantified by the standard operator norm of the unitary operators. If  $Q_1$  and  $Q_2$  are two hypotheses with unitary operators correspondingly  $U_1$  and  $U_2$  (**Definition 4**), then the distance  $\Delta Q^{12} = \Delta U^{12}$  is defined as follows:

$$\Delta Q^{12} = \|U_1 - U_2\|. \quad (75)$$

According to the *genetic algorithms'* terminology, the distance in the hypothesis representation space is called *genotypes* distance.

To introduce distance in the fitness space, we note that the unitary HQMMs representations are defined in a larger Hilbert space (by tensoring an emission system) and use a *stabilized* version of the trace norm known as *diamond norm* [65]:

$$\|\mathcal{T}\|_{\diamond} = \max_{\rho \in D(\mathcal{H}_S \otimes \mathcal{H}_S)} \|(\mathcal{T} \otimes I_N)\rho\|_1. \quad (76)$$

In the diamond norm definition the dimension of the emission system  $M$  is equal to the dimension of the state system  $N$ , since the increase of  $M > N$  cannot increase the trace norm. The diamond norm induces distance between the probabilities of 1-symbol sequences generated by the hypotheses  $Q_1$  and  $Q_2$  :

$$\begin{aligned} \Delta \mathcal{T}^{12} &= \|\mathcal{T}^1 - \mathcal{T}^2\|_{\diamond} \\ &= \max_{\rho \in D(\mathcal{H}_S \otimes \mathcal{H}_S)} \|(\mathcal{T}^1 - \mathcal{T}^2) \otimes I_N \rho\|_1, \end{aligned}$$

which we call a *phenotypes* distance. Since the diamond norm is a stabilized version of the trace norm (Lemma 12, [65]) we have the inequality:

$$\|(\mathcal{T}^1 - \mathcal{T}^2)\|_1 \leq \|\mathcal{T}^1 - \mathcal{T}^2\|_{\diamond}, \quad (77)$$

and from inequality (70) follows, that the average divergence between the hypothesis  $Q_1$  and  $Q_2$  on finite sample of sequences with length 1 is a lower bound of the diamond norm:

$$\Delta_1(D^1 \| D^2) \leq \|\mathcal{T}^1 - \mathcal{T}^2\|_{\diamond}. \quad (78)$$

The introduced distances in hypothesis and fitness spaces imply smooth fitness landscape for the single-symbol sequences, due to the Continuity of Stinespring's representation Theorem [40]. According to the Theorem, two quantum operations  $\mathcal{T}^1, \mathcal{T}^2$ , respectively two QHMMs, are close in diamond norm iff they have unitary representations which are close in operator norm:

$$\frac{1}{2} \Delta \mathcal{T}^{12} \leq \Delta U^{12} \leq \sqrt{\Delta \mathcal{T}^{12}} \quad (79)$$

This inequality suggests that the operator norm difference between the hypotheses dominates the trace (77) and average (78) empirical divergences of their single-symbol distributions:

$$\frac{1}{2} \Delta_1(D^1 \| D^2) \leq \frac{1}{2} \|\mathcal{T}^1 - \mathcal{T}^2\|_1 \leq \Delta U^{12}. \quad (80)$$

The distributions over sequences with any finite length  $n$  are generated by the  $n$ -th powers of the quantum operations (35) and their unitary dilations:

$$(\mathcal{T}^i)^n \rho_0 = U_i^n \rho_0 U_i^{\dagger n}, \rho_0 \in D(\mathcal{H}_S), i \in 1, 2. \quad (81)$$

The operator-norm distance between the unitary operators defining  $n$ -symbol sequences is related to the genotypes' distance  $\Delta Q^{12} = \|U_1 - U_2\|$  as follows:

$$\begin{aligned} \|U_1^n - U_2^n\| &= \left\| (U_1 - U_2) \sum_{k=1}^n U_1^{n-k} U_2^{k-1} \right\| \\ &\leq \|U_1 - U_2\| \left\| \sum_{k=1}^n U_1^{n-k} U_2^{k-1} \right\| \\ &\leq \|U_1 - U_2\| \left( \sum_{k=1}^n \|U_1^{n-k} U_2^{k-1}\| \right) \\ &\leq n \|U_1 - U_2\|. \end{aligned} \quad (82)$$

For the case of quantum operations defining  $n$ -symbol sequences, and accounting that the diamond norm is stabilized trace norm, from the Continuity Theorem (80) follows:

$$\frac{1}{2} \|(\mathcal{T}^1)^n - (\mathcal{T}^2)^n\|_1 \leq \|U_1^n - U_2^n\|. \quad (83)$$

By applying (82) and (60),(61) to (83) we can derive an upper bound estimate for the  $n$ -symbol distributions divergence in terms of genotypes' distance in the hypothesis space :

$$\frac{1}{2n} \Delta_n(D^1 \| D^2) \leq \frac{1}{2n} \|\mathcal{T}_1^n - \mathcal{T}_2^n\|_1 \leq \Delta U^{12} \quad (84)$$

The empirical divergence of a learning sample of sequences with lengths up to  $n$  is bounded as follows:

$$\frac{1}{2n} \sum_{i=1}^n \frac{1}{i} \Delta_i(D^1 \| D^2) \leq \Delta U^{12} \quad (85)$$

This inequality allows the precision component in the fitness distance between of two hypotheses to be estimated by the operator norm distance of their unitary representations(62) :

$$\Delta_{\leq n}(D^1 \| D^2) = \frac{1}{n} \sum_{i=1}^n \Delta_i(D^1 \| D^2) \quad (86)$$

By replacing the harmonic weight  $\frac{1}{i}$  of the divergence in (85) by  $\frac{1}{n}$  and applying (86):

$$\Delta_{\leq n}(D^1 \| D^2) \leq \sum_{i=1}^n \frac{1}{i} \Delta_i(D^1 \| D^2)$$

we derive the estimate:

$$\frac{1}{2n} \Delta_{\leq n}(D^1 \| D^2) \leq \Delta U^{12} \quad (87)$$

Inequality (87) demonstrates that the fitness landscape of the QHMMs learning problem is smooth: for every two unitary hypothesis close in genotype distance (operator norms) the corresponding phenotypes' distance (empirical distributions divergence) for any sequences length  $n$  is restricted.

To experimentally investigate the difficulty of the heuristic approach to the QHMM learning task we estimate the landscape properties of the the QHMM learning problem discussed in Example 3. The dependency between the change in the operator norm and the corresponding divergence of the sequence distributions is estimated by a random walk starting at the optimal hypothesis  $Q^*$  with unitary  $U^* = U_0$ . A new unitary is generated at every step  $t = 1, 2, \dots$  by random single parameter mutation with standard deviation 10%. The expected fitness divergences (phenotypes distance)  $\Delta_n(D^* \| D^t)$  (61) for

sequences with lengths  $n \in [2 \dots 5]$ , and the expected total fitness divergence  $\Delta_{\leq 5}(D^* \| D^t)$  (86) conditioned on the genotypes distance (75)  $\Delta U = \|U^* - U_t\|, \Delta U \in [0, 1]$  are shown on FIG 11.

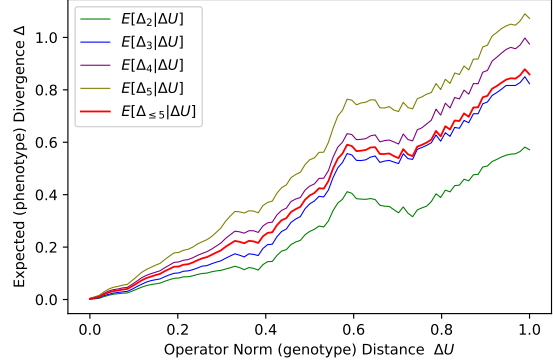


FIG. 11. Smoothness of Fitness Landscape

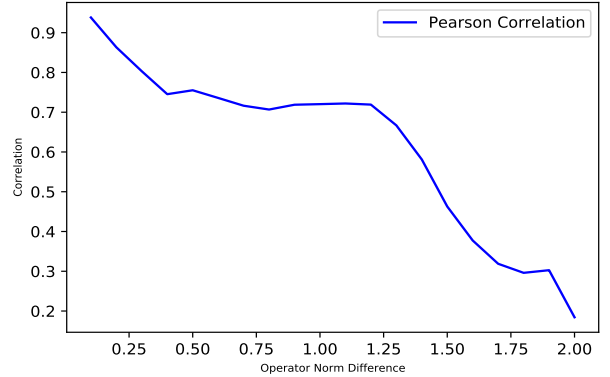


FIG. 12. Correlation of Fitness Landscape

On FIG 12 we present estimations of the Pearson correlation coefficient of the fitness of a hypothesis and its distance to the optimal solution for sequences with length up to 5 symbols:

$$r = \frac{\text{cov}(\Delta_{\leq 5}(D^* \| D^t), \Delta U)}{\text{std}(\Delta_{\leq 5}(D^* \| D^t))\text{std}(\Delta U)} \quad (88)$$

The coefficient is estimated for three mutation rates and can be used as measure of the expected effectiveness of the evolutionary algorithms applied to the QHMM learning problem.

#### IV.E. QHMM Learning Algorithm

The learning algorithm takes as input an estimation of the Hankel matrix associated with the unknown process language  $\hat{H}^L \in R^{\Sigma^{\leq n} \times \Sigma^{\leq n}}$  and the specification of a hypothesis space  $\mathbb{Q}$ . Two of the components of the hypothesis space are fixed by the Hankel matrix  $\hat{H}^L$ : the alphabet  $\Sigma$  and the dimension of the state Hilbert space  $\mathcal{H}_S$  which is  $\hat{N} = \text{rank}(\hat{H}^L)$ . The free parameters, subject of optimization, are the dimension  $M$  of the emission Hilbert space  $\mathcal{H}_E$ , the unitary  $U$ , the mapping  $\mathcal{M}$ , and the type of the initial density  $\rho_0$ . In order to simplify the discussion and focus on the essential part of the algorithm, we will assume that only the unitary transformation  $U$  will be learned.

The hypothesis space  $\mathbb{Q}$  comprises both discrete and continuous components, represented by structural and parametric subspaces. The structural subspace contains the non-parametric parts  $g = \langle (t), (q), (\cdot) \rangle$  of the linear quantum circuits'  $\{\mathcal{C}_U\}$  as defined in (57). The parametric subspace is defined by vectors  $\{\mathcal{P}_U\}$  with circuit gates' parameters:

$$\mathcal{P}_U = \{p : \exists g \in \mathcal{C}_U, g = \langle (\cdot), (\cdot), (p) \rangle\}.$$

The algorithm performs evolutionary global search in the structural subspace as the fitness of every circuit structure is estimated by parametric optimization of (72):

$$Fit(\mathcal{C}_U) = \max_{\mathcal{P}_U} F(Q_U), \quad (89)$$

where  $\mathcal{C}_U$  is the unitary encoding of the hypothesis  $Q_U$ . The optimal parameters  $P_U^* = \underset{\mathcal{P}_U}{\text{argmax}} F(Q_U)$  of every hypothesis  $Q_U$  are calculated by local multivariate nonlinear optimization procedure. Derivative-free solvers as *Powell, TNC, Cobyla* as well as gradient-based *BFSG, GC, SLSQP* have been used. The type of solver for each structure optimization is selected by an adaptive local search optimization procedure. After the optimization the optimal parameters  $P_U^*$  become parameters of the hypothesis and the optimal fitness value becomes fitness of the hypothesis. The combination of evolutionary global search in the space of quantum circuit structures and local parametric optimization classifies our learning method as *Lamarckian learning* [66].

The algorithm starts with random generation of a finite sample of  $\mu$  hypotheses forming the initial *population* (Algorithm 2). The process of iterative improvement of the population consists of three base randomized steps, including selection of set of existing hypotheses to be improved referred to as parents, modification of the parents to gen-

---

#### Algorithm 2: Random Hypothesis

---

```

procedure RANDOMGATE( $\mathbb{Q}$ )
   $t \sim \text{gatesDistribution}(\mathcal{G})$ 
  /* Select gate's type */
   $q_c, q_d \sim \text{qubitsDistribution}(N, M)$ 
  /* Select control and data qubits */
   $p_1, p_2 \sim \text{parametersDistribution}([0, 8\pi])$ 
  /* Select gate parameters */
   $gate \leftarrow \langle t, (q_c, q_d), (p_1, p_2) \rangle$ 
  /* Create a gate */
  return  $gate$ 

procedure RANDOMHYPOTHESIS( $\mathbb{Q}$ )
   $minGts, maxGts \leftarrow const_1, const_2$ 
  /* Min-Max number of gates */
   $numGts \sim \text{Uniform}(minGts, maxGts)$ 
  /* Random number of gates */
   $\mathcal{C} \leftarrow []$ 
  /* Initial circuit for the hypothesis */
  for  $g = 1$  to  $numGts$  do
     $\mathcal{C} \leftarrow \mathcal{C} + [\text{RANDOMGATE}(\mathbb{Q})]$ 
   $\mathcal{P}_C^* \leftarrow \underset{\mathcal{P}_C}{\text{argmax}} F(\mathcal{C})$  /* Find parameters
   $\mathcal{P}_C^*$  of  $\mathcal{C}$  which maximize the fitness */
   $F_C \leftarrow F(\mathcal{C}^*)$  /* Fitness value of  $\mathcal{C}^*$  */
  return  $\mathcal{C}^*$ 

```

---

erate offspring or children, selection from the parents and children a new generation of the population (Algorithm 3). The modification operations include range of hypothesis mutations (Algorithm 4) utilized by a stochastic local search (Algorithm 5). Since the random operations selecting offspring and survivors are biased towards hypotheses with higher fitness (*survival of the fittest*), the entire population evolves towards regions of the space  $\mathbb{Q}$  which contain better potential solutions and eventually an optimal solution. The trade-off between exploration and exploitation within a hypothesis space region is controlled by a global variable referred to as *Temperature*. The temperature defines the probability of accepting a new hypothesis, even if it is not superior to its parent. The temperature gradually decreases with the search progression, thereby increasing the likelihood of selecting only better solutions. If a certain threshold of steps is reached without any fitness improvement, the temperature is reset to its highest value to allow exploration of new regions. The temperature( $\tau$ ) is calculated as a function of the number of steps  $t$  (FIG (13)) as follows:

$$\tau = (t^{\frac{3}{2}} + 1)^{-\frac{1}{4}}.$$

The probability a new hypothesis with fitness  $F_{new}$  to be accepted instead of its superior parent

**Algorithm 3: Evolutionary Learning**


---

**Input** :  $\mu, \lambda, \mathbb{Q}$  (56),  $F(Q)$  (72),  $F^*$ ,  $gMax$ ,  $\mathcal{G}$   
**Output**: Best Hypothesis  $Q^* = \operatorname{argmax}_{Q \in \mathbb{Q}} F(Q)$

**Initialize**

- $g \leftarrow 0$  /\* Evolutionary generation \*/
- $t \leftarrow 0$  /\* Search progress steps \*/
- $P_g \leftarrow \text{RANDOM}(\mu, \mathbb{Q})$  /\* Initial population:  $\mu$  random hypotheses \*/

**while**  $\max_{Q \in P_g} F(Q) < F^*$  and  $g < gMax$  **do**

$\tau \leftarrow \text{Temperature}(t)$   
 $Parents \leftarrow \text{Select}(P_g, \lambda, \text{selectionDistribution})$   
 $Children \leftarrow \text{Modify}(Parents, \tau, \text{modificationDistributions})$   
 $P_{g+1} \leftarrow \text{Select}(P_g \cup Children, \mu, \text{survivalDistribution})$   
 $g \leftarrow g + 1$   
/\* Check for search progress during last progWin steps \*/  
**if** **noProgress**(progWin) **then**  
|  $t \leftarrow 0$   
**else**  
|  $t \leftarrow t + 1$   
 $Distributions \leftarrow \text{Adapt}(Distributions)$

**return**  $\operatorname{argmax}_{Q \in P_g} F(Q)$

---

**Algorithm 4: Mutate a Hypothesis**


---

**procedure** **MUTATEHYPOTHESIS**( $\mathcal{C}$ ,  $pos$ ,  $mType$ )

**switch**  $mType$  **do**

**when** "gte" :  
 $\mathcal{C}[pos].gate \sim \text{gatesDistribution}(\mathcal{G})$   
/\* Mutate gate's type \*/  
**when** "qbt" :  $\mathcal{C}[pos].qubits \sim \text{qubitsDistribution}(N, M)$  /\* Mutate gate's qubits \*/  
**when** "rpl" :  
 $\mathcal{C}[pos] \leftarrow \text{RANDOMGATE}(\mathbb{Q})$  /\* Replace gate \*/  
**when** "dlt" :  $\mathcal{C}[pos:] \leftarrow \mathcal{C}[pos + 1:]$   
/\* Delete gate \*/  
**when** "ins" :  $\mathcal{C} \leftarrow \mathcal{C}[pos] + [\text{RANDOMGATE}(\mathbb{Q})] + \mathcal{C}[pos:]$   
/\* Insert gate \*/

**return**  $\mathcal{C}$

---

**Algorithm 5: Hypothesis Modification**


---

**procedure** **MODIFYHYPOTHESIS**( $\mathcal{C}$ )

$\mathcal{C}_{best} \leftarrow \mathcal{C}$  /\* Current best hypothesis \*/  
 $\mathcal{C}_{current} \leftarrow \mathcal{C}$  /\* Current hypothesis \*/  
 $searchSteps \sim \text{localSearchLen}(1..max)$   
/\* Random local search steps \*/  
**for**  $step = 1$  **to**  $searchSteps$  **do**

$sType \sim \text{localSearchType}("depth", "breadth")$   
/\* local search type \*/  
 $mProb \sim \text{mutationRate}(0.1, \dots, 0.5)$   
/\* Mutation rate \*/  
 $\mathcal{C} \leftarrow \mathcal{C}_{current}$  /\* Current hypothesis to search around \*/

**for**  $pos = 1$  **to**  $\text{Size}(\mathcal{C})$  **do**

**if**  $\text{RANDOM} > mProb$  **then**  
 $mType \sim \text{mutationType}("gte", \dots, "ins")$   
/\* Mutation type \*/  
 $\text{MUTATEHYPOTHESIS}(\mathcal{C}, pos, mType)$   
/\* Mutate hypothesis at pos \*/

$\mathcal{P}_{\mathcal{C}}^* \leftarrow \operatorname{argmax}_{\mathcal{P}_{\mathcal{C}}} F(\mathcal{C})$  /\* Find parameters  $\mathcal{P}_{\mathcal{C}}^*$  which maximize the fitness \*/  
 $F_{\mathcal{C}} \leftarrow F(\mathcal{C})$  /\* Fitness value of  $\mathcal{C}$  with optimal parameters  $\mathcal{P}_{\mathcal{C}}^*$  \*/  
**if**  $F(\mathcal{C}) > F(\mathcal{C}_{best})$  **then**  
 $\mathcal{C}_{best} \leftarrow \mathcal{C}$  /\* Save the new best hypothesis \*/

**if**  $\text{ACCEPT}(F(\mathcal{C}), F(\mathcal{C}_{current}), Temperature)$  **then**  
 $\mathcal{C}_{current} \leftarrow \mathcal{C}$  /\* New current hypothesis \*/

**if**  $\text{ACCEPT}(F(\mathcal{C}), F(\mathcal{C}_{best}), Temperature)$  **then**  
 $\mathcal{C}_{best} \leftarrow \mathcal{C}$  /\* new preferred hypothesis \*/

**return**  $\mathcal{C}_{best}$

---

with fitness  $F_{old} \geq F_{new}$  at temperature  $\tau$  is defined by:

$$P_{new} = \exp\left(\frac{0.6}{\tau} \frac{F_{old} - F_{new}}{F_{old}}\right)$$

The control of hypothesis acceptance probability by the global temperature  $\tau$  is illustrated FIG 14.

The selection of a set of hypotheses, referred to as

parents, to be modified and evaluated as potential new members of the population relies on the fitness of these hypotheses. The candidates with better fitness are more likely to be selected for further consideration. This approach can be successful in case of unimodal landscapes. However, if the fitness landscape is rugged, characterized by numerous local extrema, employing a uniform, strong selection pres-

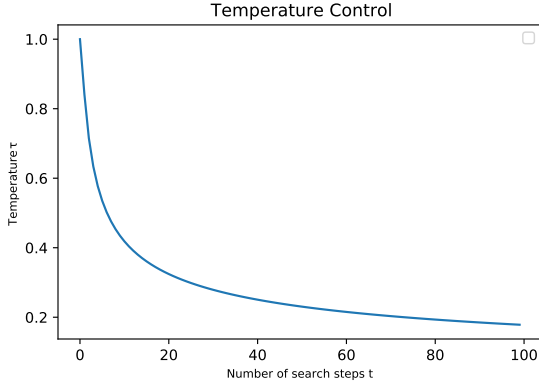


FIG. 13. Temperature control

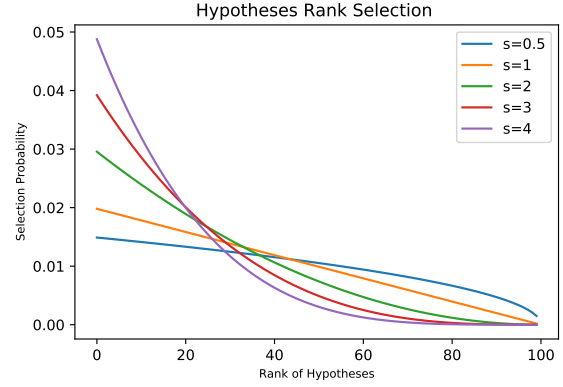


FIG. 15. Rank Selection Distributions

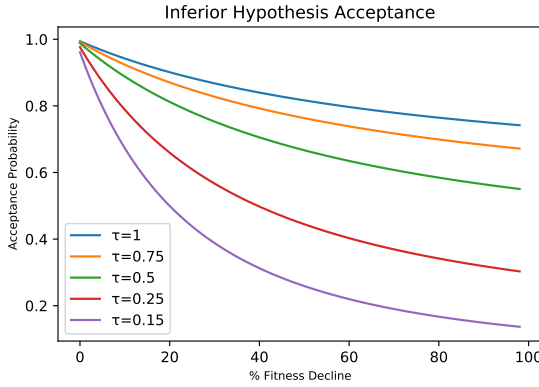


FIG. 14. Inferior Hypotheses Acceptance

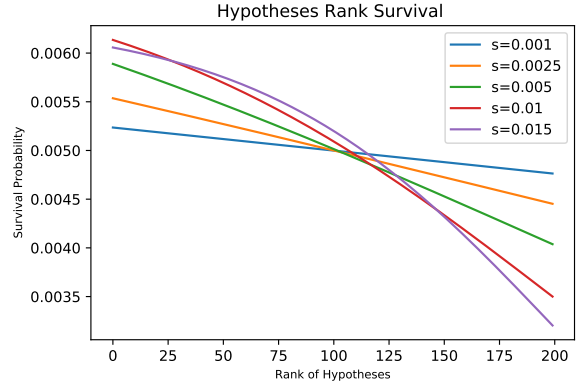


FIG. 16. Rank Survival Distributions

sure strategy can result in premature convergence towards a local solution. Therefore, in our algorithm we use selection distributions based on rank, fitness, and tournaments. Every selection distribution type is used with up to 5 levels of selection pressure. For example, let's consider rank-based selection where the hypothesis are ranked according to their fitness values with the fittest hypothesis receiving the lowest rank. Then the probability a hypothesis with rank  $i$  to be selected for offspring generation is:

$$P_{selection}[Q_i] = \frac{(\mu - i)^s}{\sum_{r=1}^{\mu} (\mu - r)^s},$$

where  $\mu$  is the size of the population and  $s$  is a parameter called *selection strength*. The shape of the rank selection distribution for different values of the parameter is shown on FIG 15.

The survival distributions define the chance a hypothesis - old or newly generated- to participate in the new generation. These distributions are also based on rank and fitness and use up to 5 levels of selection pressure. The probability a hypothesis

with rank  $i$  to be selected to 'survive' in the next generation is:

$$P_{survival}[Q_i] = \frac{(d_i + 1)^{-1}}{\sum_{r=1}^{\mu} (d_r + 1)^{-1}}, \quad (90)$$

where

$$d_r = \exp\{s(r - \mu - \lambda)\}, \quad (91)$$

$\mu$  is the size of the population,  $\lambda$  is the size of the offspring, and  $s$  is a parameter called *survival strength*. The shape of the rank survival distribution for different values of the parameter is shown on FIG 16.

The evolutionary algorithm uses multiple distributions to implement the processes of selection, modification, and survival (TABLE III). The parameters of these distributions along with the population size  $\mu$  and the offspring size  $\lambda$  are referred to as *hyperparameters* of the algorithm. The hyperparameters are critical for the performance of the algorithm. Since each learning task is unique and the fitness landscape can change during the evolutionary process, it is essential to dynamically adjust the

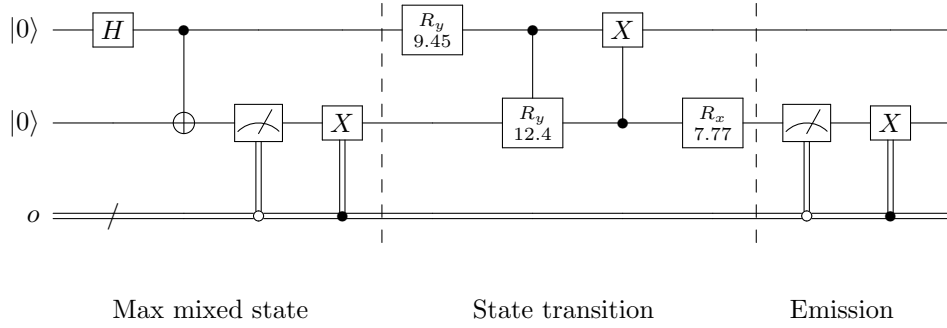


FIG. 17. QHMM Defining Market Distribution

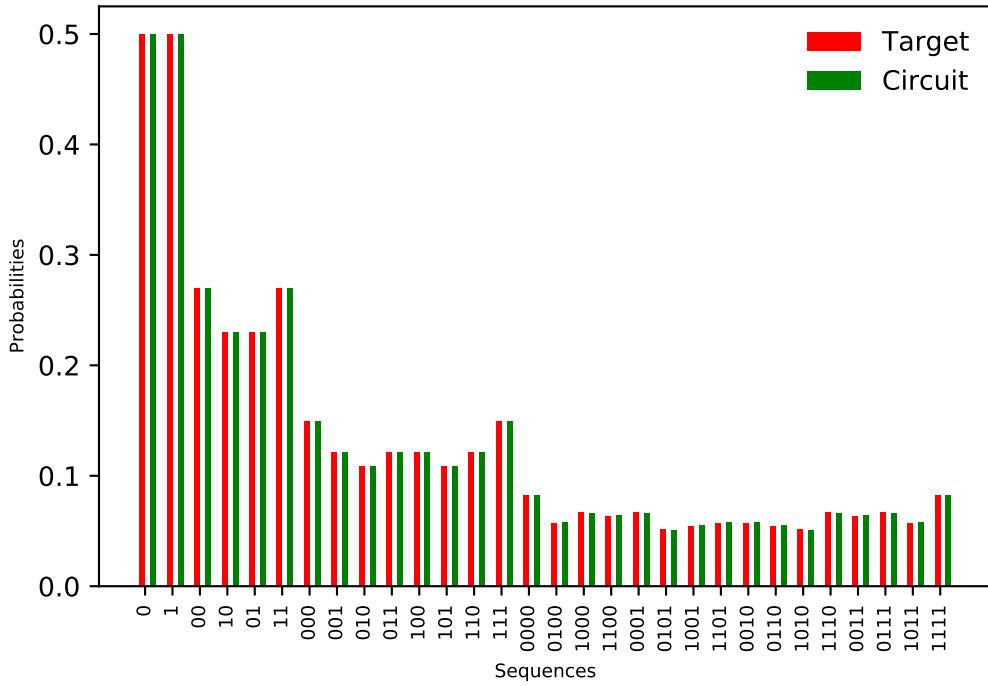


FIG. 18. Targeted and Learned Market Distributions

hyperparameters as the learning evolves. To achieve adaptive control over the hyperparameters, we employ a reinforcement learning algorithm based on the "multi-armed bandit model". This algorithm effectively addresses the exploration-exploitation trade-off, and maximizes the cumulative reward obtained through the parameters adaptation. Let's assume that the evolutionary algorithm utilizes a procedure or distribution  $A(h)$  which depends on a parameter

$h \in \{h_1, \dots, h_k\}$ . For a generation  $t$  we define a distribution  $D_t^h = \{p_i : p_i = P[h_i]\}$ . Every time when  $A$  is used during the generation  $t$  we first sample a value  $h \sim D_t^h$  and then use it for this particular activation  $A(h)$ . We register if the particular usage of  $A(h)$  has been successful or not. Success is considered when the fitness of a hypothesis or a population has increased and in this case the value of  $h$  receives reward 1. In the end of the genera-



tion  $t$  we will have a reward vector  $\mathbf{r}_t = [r_t^1, \dots, r_t^k]$ , where  $r_t^j$  is the number of times the usage of the value  $h = h_j$  during the generation  $t$  has resulted in fitness improvement. Let the initial distribution be the uniform distribution  $D_0^h = \{\frac{1}{k}, \dots, \frac{1}{k}\}$ . The distribution at generation  $t + 1$  is defined as follows:

$$D_{t+1}^h = \left\{ p_i : p_i = \gamma \frac{1}{k} + (1 - \gamma) \frac{r_t^i}{\sum_{j=1}^k r_t^j}, i = [1, k] \right\},$$

where  $\gamma \in [0, 1]$  quantifies the trade-off between exploration and exploitation. The pseudo code of the algorithm is presented as Algorithm 3.

**Example 3.** In this example we apply the QHMM learning algorithm to the Market classical HMM discussed in **Example 1**. The minimal order of the classical model estimated using the Hankel matrix is:  $n = 4$ . The learning sample as distributions of sequences with lengths up to  $t = 2n - 1 = 7$  was generated using the string function of the classic model (EQ 6). The QHMM sequences distribution is generated using the sequence function (EQ 6). The preliminary model specification based on the learning sample analysis is the following:

$$\mathbf{Q} = \{\Sigma, \mathcal{H}_S, \mathcal{H}_E, U, \mathcal{M}, \rho_0\}$$

where  $\Sigma = \{0, 1\}$ ,  $\mathcal{H}_S$  is a Hilbert space with dimension  $N = \sqrt{n} = 2$  (i.e. 1 qubit quantum system),  $\mathcal{H}_E$  is a Hilbert space with dimension 2 (i.e. 1 qubit quantum system and the measurement basis is  $\{|0\rangle, |1\rangle\}$ ),  $U$  is a unitary operation on the Hilbert space  $\mathcal{H}_E \otimes \mathcal{H}_S$  implemented by quantum gates in  $\mathcal{G} = \{X, Y, RX, RY\}$ , and  $\rho_0$  is the tensor product of uniformly distributed state and grounded emission systems.

Exact match (i.e zero-divergence between classic and quantum distributions) was reached in average of 150 iterations by population of 100 solutions. The best solution is shown in FIG 17. Part of the target and learned distributions at the end of the search are shown in FIG 18.

In the next example we demonstrate that the QHMMs are efficient generators of stochastic mixtures of distributions.

**Example 4.** Let's consider a process each point of which is drawn from a Normal distribution belonging to a finite set of Normal distributions:

$$\{Y_t : Y_t \sim \mathcal{N}(\mu, \sigma^2(s), s \in S)\},$$

where  $S = \{s_1 \dots s_N\}$  is a finite set of unobservable states. The classical HMM of such a process with  $n=4$  hidden states, defining standard deviations correspondingly  $[0.5, 1, 2, 4]$  is specified in Table IV. The model is minimal and in each state

$s \in S$  an integer observable in the interval  $[0, 3]$  is emitted by sampling from a normal distribution  $\mathcal{N}(\mu = 1.5, \sigma(s))$  as shown in FIG 19. The learning sample is a set of distributions of sequences with lengths up to  $t = 2N - 1 = 7$ . It was generated using the string function of the classic model (EQ 6). The preliminary model specification based on the learning sample analysis is the following:

$$\mathbf{Q} = \{\Sigma, \mathcal{H}_S, \mathcal{H}_E, U, \mathcal{M}, \rho_0\}$$

where  $\Sigma = \{0, 1\}$ ,  $\mathcal{H}_S$  is a Hilbert space with dimension  $N = \sqrt{n} = 2$  (i.e. 1 qubit quantum system),  $\mathcal{H}_E$  is a Hilbert space with dimension 4 (i.e. 2-qubit quantum system and the measurement basis is  $\{|0, 0\rangle, |0, 1\rangle, |1, 0\rangle, |1, 1\rangle\}$ ),  $U$  is a unitary operation on the Hilbert space  $\mathcal{H}_E \otimes \mathcal{H}_S$  implemented by quantum gates in  $\mathcal{G} = \{X, Y, RX, RY, P\}$ , and  $\rho_0$  is the tensor product of maximally mixed state system and grounded emission systems. Divergence error less than 0.01% was reached in average of 250 iterations by population of 150 hypotheses. The best solution is shown in FIG 20. Part of the target and learned distributions at the end of the search are shown in FIG 21.

#### IV.F. Learning QHMM with Ansatz Circuits

In this paper we propose the following algorithm for learning *quantum hidden Markov model* using ansatz circuits.

---

**Algorithm 6:** Quantum Hidden Markov Model Learning with Ansatz Circuits

---

**Input** : table of observed sequences and corresponding probabilities, min-max sequence length (optional)

**Output:** trained circuit that can be extended to the required sequence length

- 1 Initialize start state, variational quantum circuit ansatz, start values of the parameters. Multiple options for start states and circuit ansatz are discussed in Section III B.
  - 2  $Cost = \sum_i l_i \times (p_i^{target} - p_i^{current})^2$  where  $l_i$  is the sequence length
  - 3 Find optimal parameters for quantum circuit with classical technique, e.g. Nelder–Mead method.
- 

This approach essentially utilizes the training of parameterized quantum circuits to model sequence data.

<i>Distribution</i>	Description	Domain
selectionDistributionTypes	Probabilities of selection types.	[ <i>Fitness, Rank, Tournament</i> ]
selectionDistributionStrength	Probabilities of selective pressure levels	[0.1, 0.2, 0.5, 0.7, 1]
survivalDistributionTypes	Probabilities of survival types	[ <i>Fitness, Rank</i> ]
survivalDistributionStrength	Probabilities of survival pressure levels.	[0.1, 0.2, 0.5, 0.7, 1]
gatesDistribution	Probabilities of gate types	$\mathcal{G} = \{g_0 \cdots g_k\}$
qubitsDistribution	Probabilities of qubits	$[1, n + m], P(n + m, 2)$
localSearchLen Distribution	Probabilities of local search steps	[1, 10]
localSearchType Distribution	Probabilities of local search types	[ <i>depth, breadth</i> ]
mutationRate Distribution	Probabilities of hypothesis' mutation rates	[0.1, ...0.5]
mutationType Distribution	Probabilities of hypothesis' mutation types	[ <i>'gte', 'qbt', 'rpl', 'dlt', 'ins'</i> ]
optimizationAlgs Distribution	Probabilities of nonlinear solvers	[ <i>'tnc', 'cbla', 'bfsq', 'gc', 'slsqp'</i> ]

TABLE III. Adaptive distributions used by the evolutionary algorithm

<i>S</i>	Description	<i>S</i>	0	1	2	3	<i>S</i>	0	1	2	3
0	Low Variance	0	0.60	0.25	0.05	0.10	0	0.00	0.50	0.50	0.00
1	Low-Medium Variance	1	0.05	0.15	0.05	0.75	1	0.01	0.49	0.49	0.01
2	Medium-High Variance	2	0.75	0.05	0.15	0.05	2	0.13	0.37	0.37	0.13
3	High Variance	3	0.10	0.05	0.65	0.20	3	0.22	0.28	0.28	0.22

TABLE IV. Gaussian Mixture HMM. Left: Hidden States Descriptions. Center: States Transition Probabilities. Right: Emission Probabilities.

#### IV.G. Ansatz Circuit Template

The topic of efficient ansatz selection is an area of active research [67–71]. Due to the presence of noise in quantum devices, one must select an ansatz, which is sufficiently expressive (i.e. able to access the solution space in the Hilbert space) while maintaining low parameter count and lower depth of the quantum circuits in order to suppress the noise. Moreover, the proposed ansatz should contain sufficient entanglement to be non-simulable on a classical computer. Qiskit provides a variety of built-in ansatz templates with various combinations of the number of parametric gates and the circuit depth [72]. The two ansatz circuits we test in this work are `RealAmplitudes` (FIG 22) and `EfficientSU2` (FIG 23 and FIG 24). We consider two variations for `EfficientSU2` ansatz circuit: 1) with  $R_y, R_z$  (FIG 23) and 2) with  $R_z, R_x$  (FIG 24) rotation gates. Furthermore, in the entanglement block we test full and linear entanglement schemes. The latter scheme is more hardware efficient as it doesn't assume fully connected mapping between qubits.

#### V. EXAMPLES OF QHMMS

##### V.A. Simple Four Symbol Stochastic Process

Let's consider a process defined by the following Kraus operators [25]:

$$\frac{1}{\sqrt{2}}|0\rangle\langle 0|, \frac{1}{\sqrt{2}}|1\rangle\langle 1|, \frac{1}{\sqrt{2}}|+\rangle\langle +|, \frac{1}{\sqrt{2}}|-\rangle\langle -|$$

or

$$\begin{pmatrix} \frac{1}{\sqrt{2}} & 0 \\ 0 & 0 \end{pmatrix}, \begin{pmatrix} 0 & 0 \\ 0 & \frac{1}{\sqrt{2}} \end{pmatrix}, \frac{1}{2} \begin{pmatrix} \frac{1}{\sqrt{2}} & \frac{1}{\sqrt{2}} \\ \frac{1}{\sqrt{2}} & \frac{1}{\sqrt{2}} \end{pmatrix}, \frac{1}{2} \begin{pmatrix} \frac{1}{\sqrt{2}} & -\frac{1}{\sqrt{2}} \\ -\frac{1}{\sqrt{2}} & \frac{1}{\sqrt{2}} \end{pmatrix}$$

Ansatz	Entanglement	Cost
EfficientSU2 ( $R_z, R_x$ )	full	3.90e-5
EfficientSU2 ( $R_z, R_x$ )	linear	4.23e-5
RealAmplitudes	full	0.155
RealAmplitudes	linear	0.689
EfficientSU2 ( $R_y, R_z$ )	full	0.156
EfficientSU2 ( $R_y, R_z$ )	linear	0.155

TABLE V. Optimized cost for different circuit ansatze

We will use maximally mixed state as a start state in this case. Next we model this sequence using

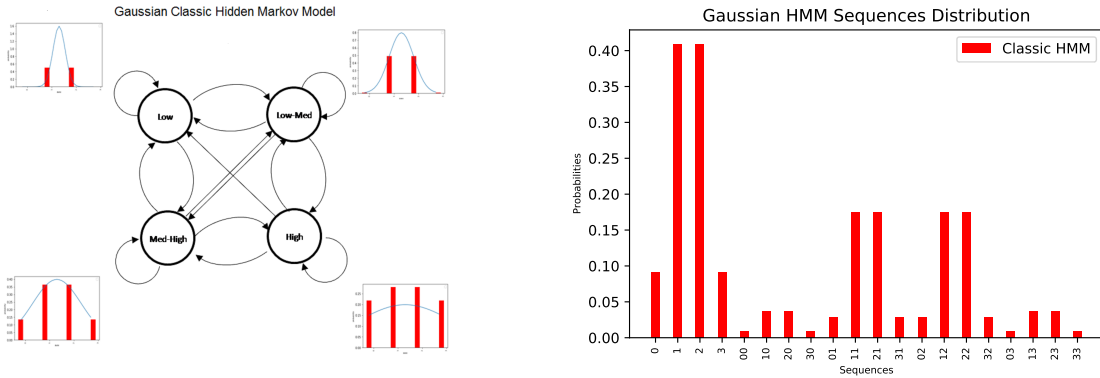


FIG. 19. Gaussian Mixture HMM

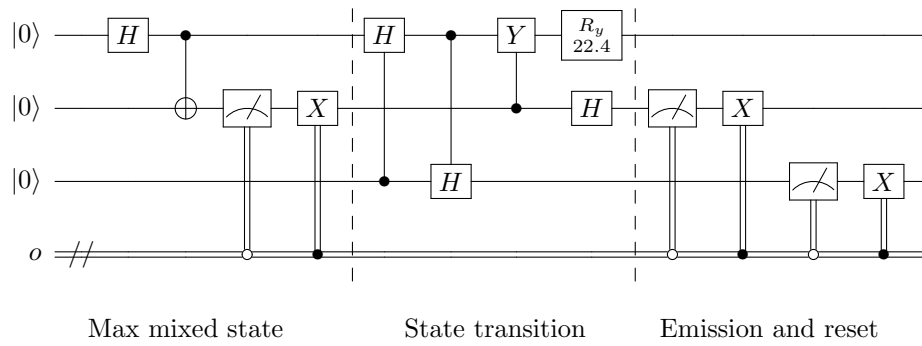


FIG. 20. Gaussian QHMM

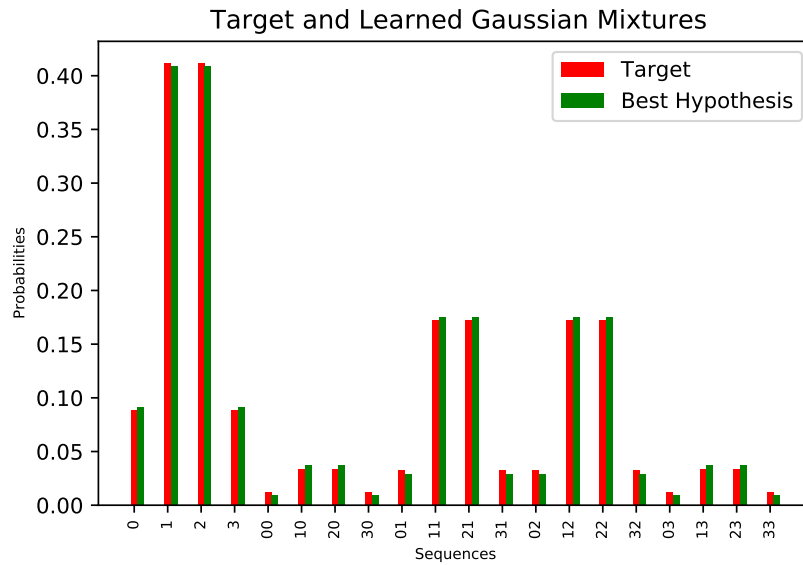


FIG. 21. Learned Gaussian Mixture

the set of ansatz circuits described in Section III B and compare different entanglement strategies that

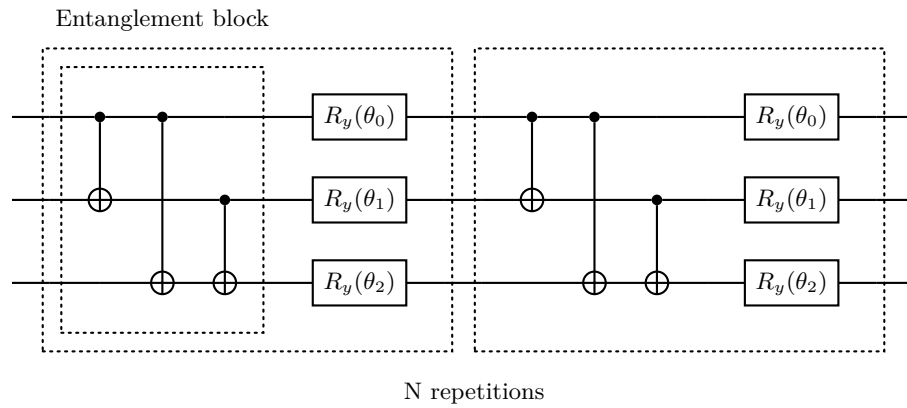
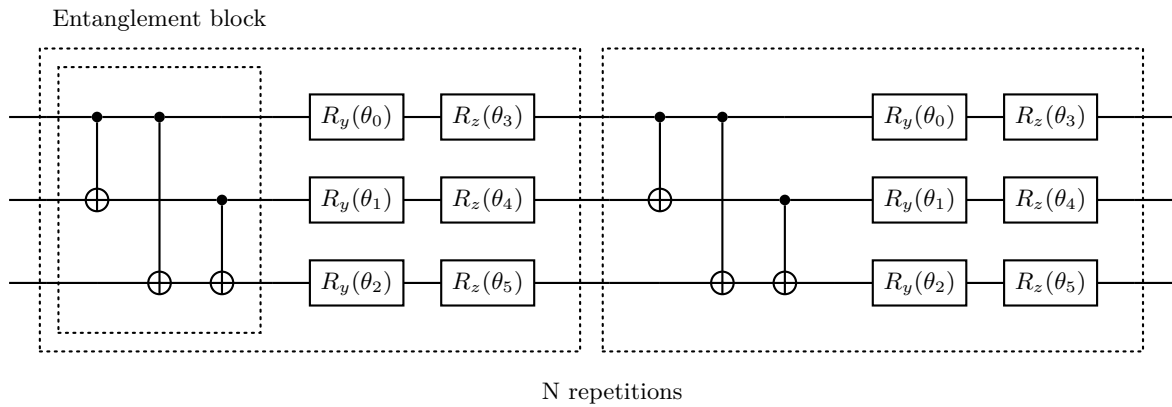
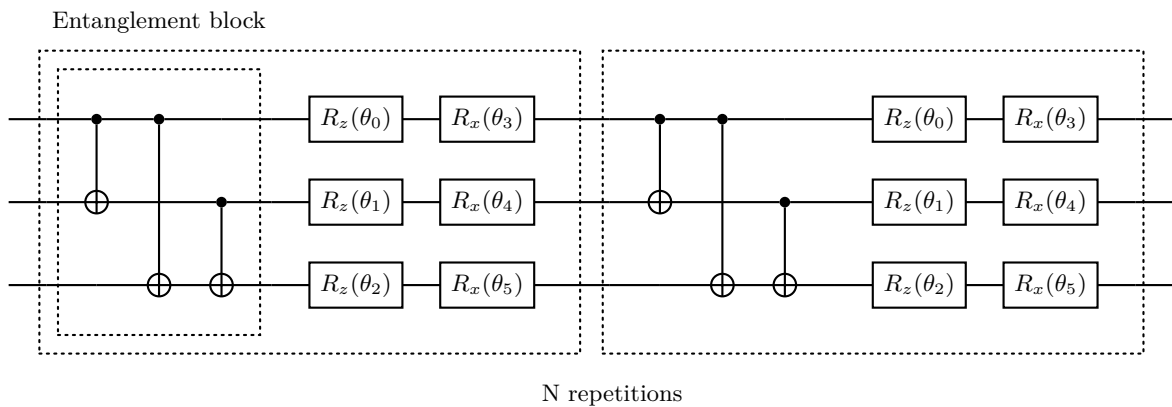


FIG. 22. Real Amplitudes Circuit Ansatz

FIG. 23. EfficientSU2 Circuit Ansatz with  $R_y$  and  $R_z$  RotationsFIG. 24. EfficientSU2 Circuit Ansatz with  $R_z$  and  $R_x$  Rotations

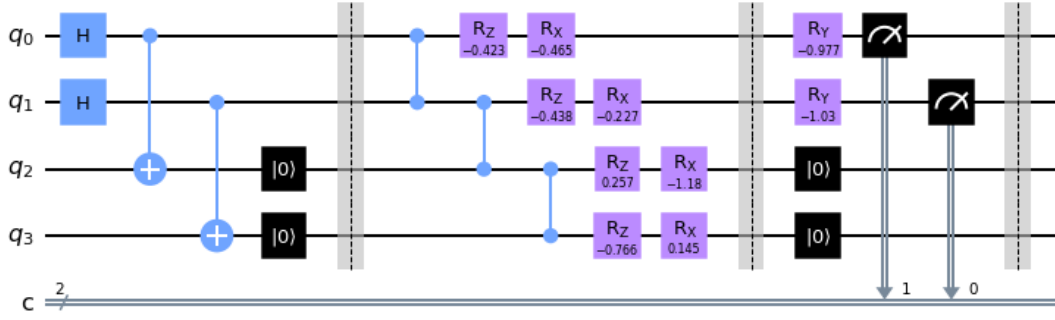


FIG. 25. Circuit for 1 step with optimized parameters

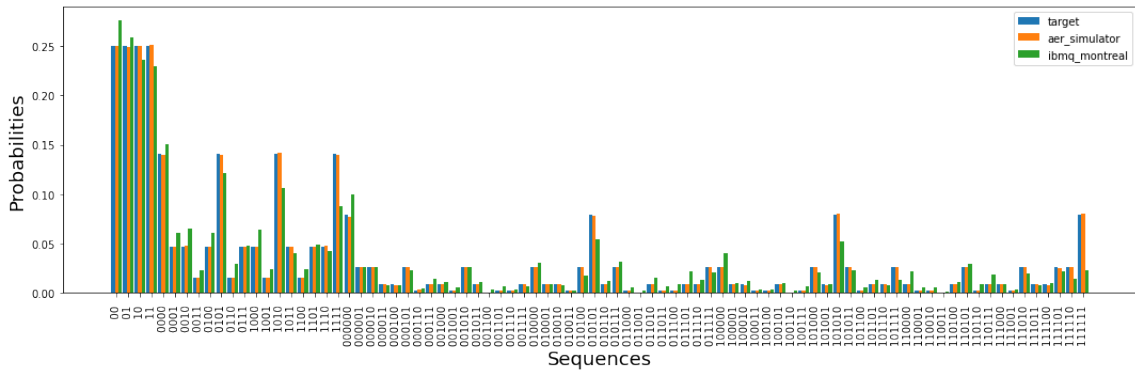


FIG. 26. Predicted and observed probabilities

include full entanglement and linear entanglement. Comparison of the results is presented in Table V.

Clearly, EfficientSU2 ( $R_z, R_x$ ) style ansatz performs much better than others. There is, however, only marginal difference between full and linear entanglement strategies. Due to heavy hex lattice used in IBM processors it is expensive to run the circuit with full entanglement on four qubits. However, we have seen that using linear entanglement produces equally good results, so we will proceed with linear entanglement design FIG 25. The result is presented on FIG 26. Hardware results [73] clearly capture the pattern. However, the current level of hardware noise still seems too high for longer sequences.

The hardware run was executed using *Sampler* primitive on *Qiskit Runtime* with *optimization\_level=2* [74, 75].

### V.B. Classic Market Model with Four Hidden States

The process is defined by transition and emission matrices in Table I.

We will simulate this process using 2 qubits: one for the principal system and one for the environment. We will use the maximally mixed state as initial state. For the main transition unitary, we will use RealAmplitudes, EfficientSU2 ( $R_y, R_z$ ) and EfficientSU2 ( $R_z, R_x$ ) circuit ansatz. Clearly, for the circuit of only 2 qubits linear and full entanglement produce the same result.

Once we train the model following Algorithm 6, we get the following costs associated with ansatz circuits (Table VI):

TABLE VI. Optimized cost for different circuit ansatz

Ansatz	Cost
EfficientSU2 ( $R_z, R_x$ )	0.00030
RealAmplitudes	0.00030
EfficientSU2 ( $R_y, R_z$ )	0.00036

Results are very close, so we can pick the simplest circuit to continue. In this case we choose RealAmplitudes since it has only 2 parameters. The circuit for 1 step with optimized parameters is shown on FIG 27.

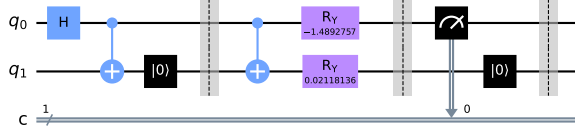


FIG. 27. Circuit for 1 step with optimized parameters

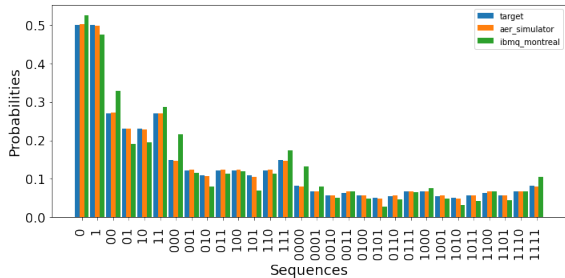


FIG. 28. Predicted and observed probabilities

Comparison with the hardware run on `ibmq_montreal` using Qiskit Runtime and Sampler primitive [76] is shown on FIG 28. The hardware run was executed using *Sampler* primitive on *Qiskit Runtime* with `optimization_level = 2` [74, 75].

The training has converged to the final solution very quickly. In fact, it is easy to see that even the RealAmplitudes ansatz is too expressive for this stochastic process and we can further simplify it by removing  $R_Y$  rotation gate on  $q_1$ .

## VI. CONCLUSIONS AND OUTLOOK

In this paper we utilized the theory of open quantum systems to study complexity, unitary implementation, and learning from examples of a class of quantum stochastic generators known as Quantum Hidden Markov Models. We have demonstrated that the integration of unitary dynamics of a principal (or “state”) quantum system, entangled with an emission system (“environment”) where observations are generated through orthogonal measurement, presents a state-efficient model of finite-order stochastic languages. The Markovian behavior of the model’s state evolution is guaranteed by the direction of the information flow from the principal system to the environment. We note that there are other quantum architectures which generate joint evolution of a Markovian state process and a dependent observable process. It is especially important to characterize the processes generated by sequential measurements of cluster state quantum systems [77], [25]. Since these systems have less free parameters - the general entanglement architecture and the parameters of the measurement basis - we would expect efficient learning algorithms.

Another important research opportunity is to apply the approach developed in the article to devices and processes with non-Markovian behavior. In this case we need to establish an information flow, or input, from the environment towards the state system [78]. This will allow to model higher-order Hidden Markov Models, finite-state transducers, and generators with attention mechanisms.

We proposed three variational ansatz circuits to be used as a starting point to model classical sequence data and tested on two use cases with 4 hidden states and 2 and 4 observed outcomes.

## VII. ACKNOWLEDGEMENTS

We thank Vaibhaw Kumar, Jae-Eun Park, Laura Schleeper, and Rukhsan UI Haq for helpful discussions at the start of this work. We would like to thank John Watrous for his comments regarding quantum channels.

The views expressed in this article are those of the authors and do not represent the views of Wells Fargo. This article is for informational purposes only. Nothing contained in this article should be construed as investment advice. Wells Fargo makes no express or implied warranties and expressly disclaims all legal, tax, and accounting implications related to this article.

- 
- [1] S. Karlin and H. Taylor, *A first course in stochastic processes*. Academic press, 2012.
- [2] R. S. Mamon and R. J. Elliott, *Hidden Markov models in finance*, vol. 4. Springer, 2007.
- [3] L. E. Baum and T. Petrie, “Statistical inference for probabilistic functions of finite state markov chains,” *The annals of mathematical statistics*, vol. 37, no. 6, pp. 1554–1563, 1966.
- [4] L. R. Rabiner, “A tutorial on hidden markov models and selected applications in speech recognition,” *Proceedings of the IEEE*, vol. 77, no. 2, pp. 257–286, 1989.
- [5] A. Anandika, S. P. Mishra, and M. Das, “Review on usage of hidden markov model in natural language processing,” in *Intelligent and Cloud Computing: Proceedings of ICICC 2019, Volume 1*, pp. 415–423, Springer, 2021.
- [6] F. Lefèvre, “Non-parametric probability estimation for hmm-based automatic speech recognition,” *Computer Speech & Language*, vol. 17, no. 2-3, pp. 113–136, 2003.
- [7] K. L. Mangi Kang, Jaelim Ahn, “Opinion mining using ensemble text hidden markov models for text classification,” *Expert Systems with Applications*, vol. 94, pp. 218–227, 2018.
- [8] T. M. Porter and M. Hajibabaei, “Profile hidden markov model sequence analysis can help remove putative pseudogenes from dna barcoding and metabarcoding datasets,” *BMC bioinformatics*, vol. 22, no. 1, p. 256, 2021.
- [9] C. Yau, O. Papaspiliopoulos, G. Roberts, and C. Holmes, “Nonparametric hidden markov models with application to the analysis of copy-number-variation in mammalian genomes,” *J R Stat Soc Series B Stat Methodol*, vol. 73, no. 1, pp. 37–57, 2011.
- [10] A. Krogh, M. Brown, I. Mian, K. Sjölander, and D. Haussler, “Hidden markov models in computational biology. applications to protein modeling.,” *J Mol Biol*, vol. 235, no. 5, pp. 1501–1531, 1994.
- [11] J. M. Lee, S.-J. Kim, Y. Hwang, and C.-S. Song, “Diagnosis of mechanical fault signals using continuous hidden markov model,” *Journal of Sound and Vibration*, vol. 276, no. 3-5, pp. 1065–1080, 2004.
- [12] K. D. Ullah I, Ahmad R, “A prediction mechanism of energy consumption in residential buildings using hidden markov model,” *Energies*, vol. 11, no. 2, pp. 1–20, 2018.
- [13] Y. Yuan and G. Mitra, “Market regime identification using hidden markov models,” *SSRN Electronic Journal*, 2019.
- [14] L. E. Baum, T. Petrie, G. Soules, and N. Weiss, “A maximization technique occurring in the statistical analysis of probabilistic functions of markov chains,” *The annals of mathematical statistics*, vol. 41, no. 1, pp. 164–171, 1970.
- [15] L. E. Baum *et al.*, “An inequality and associated maximization technique in statistical estimation for probabilistic functions of markov processes,” *Inequalities*, vol. 3, no. 1, pp. 1–8, 1972.
- [16] P. J. Bickel, Y. Ritov, and T. Ryden, “Asymptotic normality of the maximum-likelihood estimator for general hidden markov models,” *The Annals of Statistics*, vol. 26, no. 4, pp. 1614–1635, 1998.
- [17] L. A. Kontorovich, B. Nadler, and R. Weiss, “On learning parametric-output hmms,” in *International Conference Machine Learning*, pp. 702–710, 2013.
- [18] S. A. Terwijn, “On the learnability of hidden markov models,” in *International Colloquium on Grammatical Inference*, pp. 261–268, Springer, 2002.
- [19] B. Ghojogh, F. Karray, and M. Crowley, “Hidden markov model: Tutorial,” 2019.
- [20] B. Anderson, “The realization problem for hidden markov models,” *Mathematics of Control, Signals and Systems*, vol. 12, no. 1, pp. 80–120, 1999.
- [21] D. Hsu, S. M. Kakade, and T. Zhang, “A spectral algorithm for learning hidden markov models,” *Journal of Computer and System Sciences*, vol. 78, no. 5, pp. 1460–1480, 2012.
- [22] B. Balle, X. Carreras, F. M. Luque, and A. Quattoni, “Spectral learning of weighted automata,” *Machine learning*, vol. 96, no. 1, pp. 33–63, 2014.
- [23] H. Jaeger, “Observable operator models for discrete stochastic time series,” *Neural computation*, vol. 12, no. 6, pp. 1371–1398, 2000.
- [24] M. A. Nielsen and I. L. Chuang, *Quantum Computation and Quantum Information: 10th Anniversary Edition*. Cambridge University Press, 2010.
- [25] A. Monras, A. Beige, and K. Wiesner, “Hidden quantum markov models and non-adaptive read-out of many-body states,” *Applied Mathematical and Computational Sciences*, vol. 3, no. 1, pp. 93–122, 2011.
- [26] S. Srinivasan, G. Gordon, and B. Boots, “Learning hidden quantum markov models,” 2017.
- [27] S. Srinivasan, C. Downey, and B. Boots, “Learning and inference in hilbert space with quantum graphical models,” 2018.
- [28] S. Adhikary, S. Srinivasan, and B. Boots, “Learning quantum graphical models using constrained gradient descent on the stiefel manifold,” 2019.
- [29] S. Adhikary, S. Srinivasan, G. Gordon, and B. Boots, *Expressiveness and Learning of Hidden Quantum Markov Models*, vol. 108 of *Proceedings of Machine Learning Research*, pp. 4151–4161. PMLR, 26–28 Aug 2020.
- [30] S. Srinivasan, S. Adhikary, J. Miller, B. Pokharel, G. Rabusseau, and B. Boots, “Towards a trace-preserving tensor network representation of quantum channels,” *Second Workshop on Quantum Tensor Networks in Machine Learning, 35th Conference on Neural Information Processing Systems (NeurIPS 2021)*, 2021.
- [31] S. Srinivasan, S. Adhikary, J. Miller, G. Rabusseau, and B. Boots, “Quantum tensor networks, stochastic processes, and weighted automata,” 2020.
- [32] S. Srinivasan, *Quantum-inspired Machine Learning with Hidden Quantum Markov Models and Tensor Networks*. PhD thesis, University of Washington,



- 2022.
- [33] B. O’Neill, T. M. Barlow, D. Šafránek, and A. Beige, “Hidden quantum markov models with one qubit,” *AIP Conference Proceedings*, vol. 1479, no. 1, pp. 667–669, 2012.
- [34] L. A. Clark, W. Huang, T. M. Barlow, and A. Beige, “Hidden quantum markov models and open quantum systems with instantaneous feedback,” in *ISCS 2014: Interdisciplinary Symposium on Complex Systems*, pp. 143–151, Springer, 2015.
- [35] M. A. Javidian, V. Aggarwal, and Z. Jacob, “Learning circular hidden quantum markov models: A tensor network approach,” *arXiv preprint arXiv:2111.01536*, 2021.
- [36] M. Cholewa, P. Gawron, P. Głomb, and D. Kurzyk, “Quantum hidden markov models based on transition operation matrices,” *Quantum Information Processing*, vol. 16, no. 4, pp. 1–19, 2017.
- [37] T. J. Elliott, “Memory compression and thermal efficiency of quantum implementations of nondeterministic hidden markov models,” *Phys. Rev. A*, vol. 103, p. 052615, May 2021.
- [38] C. Blank, D. K. Park, and F. Petruccione, “Quantum-enhanced analysis of discrete stochastic processes,” *npj Quantum Information*, vol. 7, no. 1, pp. 1–9, 2021.
- [39] W. F. Stinespring, “Positive functions on  $C^*$ -algebras,” *Proceedings of the American Mathematical Society*, vol. 6, no. 2, p. 211–216, 1955.
- [40] D. Kretschmann, D. Schlingemann, and R. F. Werner, “A continuity theorem for stinespring’s dilation,” *Journal of Functional Analysis*, vol. 255, no. 8, pp. 1889–1904, 2008.
- [41] H. Jaeger, “Observable operator models for discrete stochastic time series,” *Neural Computation*, vol. 12, no. 6, pp. 1371–1398, 2000.
- [42] J. Carlyle and A. Paz, “Realizations by stochastic finite automata,” *Journal of Computer and System Sciences*, vol. 5, no. 1, pp. 26–40, 1971.
- [43] B. Anderson, “The realization problem for hidden markov models,” *Mathematics of Control, Signals and Systems volume*, vol. 12, pp. 80–120, 1999.
- [44] Q. Huang, R. Ge, S. Kakade, and M. Dahleh, “Minimal realization problem for hidden markov models,” in *2014 52nd Annual Allerton Conference on Communication, Control, and Computing (Allerton)*, pp. 4–11, 2014.
- [45] M. Vidyasagar, “The realization problem for hidden markov models: The complete realization problem,” in *Proceedings of the 44th IEEE Conference on Decision and Control*, pp. 6632–6637, 2005.
- [46] E. Sontag, “On some questions of rationality and decidability,” *Journal of Computer and System Sciences*, vol. 11, pp. 375–381, Dec. 1975.
- [47] J.-P. Bouchaud, J. Bonart, J. Donier, and M. Gould, *Trades, Quotes and Prices: Financial Markets Under the Microscope*. Cambridge University Press, 2018.
- [48] I. Bengtsson and K. Życzkowski, *Geometry of Quantum States: An Introduction to Quantum Entanglement*. Cambridge University Press, 2 ed., 2017.
- [49] M.-D. Choi, “Completely positive linear maps on complex matrices,” *Linear Algebra and its Applications*, vol. 10, no. 3, pp. 285–290, 1975.
- [50] H.-P. Breuer and F. Petruccione, *The Theory of Open Quantum Systems*. Oxford University Press, 2007.
- [51] A. Rivas and S. F. Huelga, *Open Quantum Systems*. Springer Berlin, Heidelberg, 2012.
- [52] S. E. Smart, Z. Hu, S. Kais, and D. A. Mazziotti, “Relaxation of stationary states on a quantum computer yields a unique spectroscopic fingerprint of the computer’s noise,” *Communications Physics*, vol. 5, no. 1, p. 28, 2022.
- [53] Á. Rivas, S. F. Huelga, and M. B. Plenio, “Quantum non-markovianity: characterization, quantification and detection,” *Reports on Progress in Physics*, vol. 77, no. 9, p. 094001, 2014.
- [54] F. A. Pollock, C. Rodríguez-Rosario, T. Frauenheim, M. Paternostro, and K. Modi, “Operational markov condition for quantum processes,” *Phys. Rev. Lett.*, vol. 120, p. 040405, Jan 2018.
- [55] S. Filippov, G. Semin, and A. Pechen, “Quantum master equations for a system interacting with a quantum gas in the low-density limit and for the semiclassical collision model,” *Physical Review A*, vol. 101, no. 1, p. 012114, 2020.
- [56] J. Morris, F. A. Pollock, and K. Modi, “Non-markovian memory in ibmqx4,” *arXiv preprint arXiv:1902.07980*, 2019.
- [57] M. M. Wilde, “Preface to the second edition,” in *Quantum Information Theory*, pp. xi–xii, Cambridge University Press, nov 2016.
- [58] “Mid-circuit measurement.” <https://quantum-computing.ibm.com/lab/docs/iql/manage/systems/midcircuit-measurement/>. Accessed: 2022-11-16.
- [59] “Introduction to dynamic circuits.” <https://quantum-computing.ibm.com/admin/docs/admin/manage/systems/dynamic-circuits/Introduction-To-Dynamic-Circuits>. Accessed: 2022-11-16.
- [60] “Qiskit runtime, job cdcu23veprknk3brdl6g.” <https://quantum-computing.ibm.com/runtime/jobs/cdcu23veprknk3brdl6g>. Completed: 2022-10-27.
- [61] “Introducing new qiskit runtime capabilities — and how our clients are integrating them into their use.” <https://research.ibm.com/blog/qiskit-runtime-capabilities-integration>. Accessed: 2022-11-17.
- [62] D. Hsu, S. M. Kakade, and T. Zhang, “A spectral algorithm for learning hidden markov models,” *Journal of Computer and System Sciences*, vol. 78, no. 5, pp. 1460–1480, 2012. JCSS Special Issue: Cloud Computing 2011.
- [63] S. P. Finesso Lorenzo, Grassi Angela, “Approximation of stationary processes by hidden markov models,” *Mathematics of Control, Signals, and Systems*, vol. 22, pp. 1–22, 2010.
- [64] M. J. Kearns, *The computational complexity of machine learning*. MIT press, 1990.

- [65] D. Aharonov, A. Kitaev, and N. Nisan, “Quantum circuits with mixed states,” in *Proceedings of the thirtieth annual ACM symposium on Theory of computing*, pp. 20–30, 1998.
- [66] A. Holzinger, D. Blanchard, M. Bloice, K. Holzinger, V. Palade, and R. Rabadan, “Darwin, lamarck, or baldwin: Applying evolutionary algorithms to machine learning techniques,” in *2014 IEEE/WIC/ACM International Joint Conferences on Web Intelligence (WI) and Intelligent Agent Technologies (IAT)*, vol. 2, pp. 449–453, 2014.
- [67] S. Sim, P. D. Johnson, and A. Aspuru-Guzik, “Expressibility and entangling capability of parameterized quantum circuits for hybrid quantum-classical algorithms,” *Advanced Quantum Technologies*, vol. 2, no. 12, p. 1900070, 2019.
- [68] M. Aoki, *Notes on Economic Time Series Analysis: System Theoretic Perspectives*. Springer Berlin, Heidelberg, 1983.
- [69] Y. Du, T. Huang, S. You, M.-H. Hsieh, and D. Tao, “Quantum circuit architecture search for variational quantum algorithms,” *npj Quantum Information*, vol. 8, no. 1, pp. 1–8, 2022.
- [70] T. Haug, K. Bharti, and M. Kim, “Capacity and quantum geometry of parametrized quantum circuits,” *PRX Quantum*, vol. 2, no. 4, p. 040309, 2021.
- [71] Z. Holmes, K. Sharma, M. Cerezo, and P. J. Coles, “Connecting ansatz expressibility to gradient magnitudes and barren plateaus,” *PRX Quantum*, vol. 3, no. 1, p. 010313, 2022.
- [72] M. S. A. et al., “Qiskit: An open-source framework for quantum computing,” 2021.
- [73] “Qiskit runtime, job cdrs794godki4idpf4og.” <https://quantum-computing.ibm.com/jobs/cdrs794godki4idpf4og>. Completed: 2022-11-18.
- [74] “Configure error suppression.” [https://qiskit.org/documentation/partners/qiskit\\_ibm\\_runtime/how\\_to/error-suppression.html](https://qiskit.org/documentation/partners/qiskit_ibm_runtime/how_to/error-suppression.html). Accessed: 2022-11-21.
- [75] “Configure error mitigation.” [https://qiskit.org/documentation/partners/qiskit\\_ibm\\_runtime/how\\_to/error-mitigation.html](https://qiskit.org/documentation/partners/qiskit_ibm_runtime/how_to/error-mitigation.html). Accessed: 2022-11-21.
- [76] “Qiskit runtime, job cdtbhmge9lpogos7o1vg.” <https://quantum-computing.ibm.com/jobs/cdtbhmge9lpogos7o1vg>. Completed: 2022-11-20.
- [77] H. J. Briegel and R. Raussendorf, “Persistent entanglement in arrays of interacting particles,” *Phys. Rev. Lett.*, vol. 86, pp. 910–913, Jan 2001.
- [78] H.-P. Breuer, E.-M. Laine, and J. Piilo, “Measure for the degree of non-markovian behavior of quantum processes in open systems,” *Phys. Rev. Lett.*, vol. 103, p. 210401, Nov 2009.